N 70 12515
NASA CR 107120

Second Quarterly Report

For

PASSIVE SOLAR ARRAY ORIENTATION SYSTEM (THERMAL HELIOTROPE)

(23 March 1969 – 23 June 1969)

Contract No. NAS 5-11637
Goddard Space Flight Center
Contracting Officer: P. Videneks
Technical Monitor: John Fairbanks

Prepared by

Electrical Power Systems
Space Systems Division
Lockheed Missiles & Space Company
A Group Division of Lockheed Aircraft Corporation
Sunnyvale, California 94088

For

Goddard Space Flight Center
Greenbelt, Maryland 20771

Second Quarterly Report

For

PASSIVE SOLAR ARRAY ORIENTATION SYSTEM (THERMAL HELIOTROPE)

(23 March 1969 – 23 June 1969)

Contract No. NAS 5-11637
Goddard Space Flight Center
Contracting Officer: P. Videneks
Technical Monitor: John Fairbanks

Prepared by

Electrical Power Systems
Space Systems Division
Lockheed Missiles & Space Company
A Group Division of Lockheed Aircraft Corporation
Sunnyvale, California 94088

For

Goddard Space Flight Center
Greenbelt, Maryland 20771

SUMMARY

A. OBJECTIVE

Solar array tracking systems to date have been complex electromechanical assemblies. The objective of this program is to evaluate the feasibility of simple passive tracking concepts using bimetal elements. This evaluation includes an examination of the requirements for such devices, the development of thermal heliotrope concepts for selected requirements, analysis and design implementation of these concepts, and fabrication and testing of models of the preferred designs.

B. SCOPE OF WORK

The scope of the work for this reporting period has been to complete the general survey and concept development portions of the program. Thermal properties and model designs have also been finalized. Fabrication of test models is 75-percent complete and preliminary tests have been performed on three thermal heliotrope concepts.

C. CONCLUSIONS AND RECOMMENDATIONS

The following conclusions and recommendations are made and discussed in the text of this report:

- Angular impulse limitations on some vehicles may dictate a nonincremental tracking device.
- Bimetal elements appear to be extremely resistant to thermal cycling damage.
- Bimetal coil linear motion may be negated by use of a "non-helical helix". Coil winding diameters may also be minimized with this device.
- A continuous tracking device has been designed to supply more than adequate tracking torque by utilizing two motor coils; one coil is cooling while the other is providing tracking torque.

Progress to date has shown feasibility of the thermal heliotrope sun tracker concept. Four tracking concepts have been chosen for model fabrication and testing. Preliminary testing of three of these models has indicated functionability of the concepts.

During the next quarter a fourth model will be fabricated and the model group final tested. The test results will be analyzed and recommendations presented.

CONTENTS

ILLUSTRATIONS

SECTION I
INTRODUCTION

A. ABSTRACT

The object of this document is to report the progress of the second three-month period of a nine-month study to evaluate the feasibility of thermally actuated sun-tracking systems. These systems use bimetal elements for both sensing and motive power.

The project concerns itself with exploring the feasibility of providing solar array sun-tracking capability through the use of non-electrical devices. It consists of five main tasks.

- Survey general tracking requirements such as rate and torque requirements
- Study thermal heliotrope operating mechanisms and develop concepts
- Analyze thermal properties and provide conceptual designs
- Fabricate and test models in simulated orbit environments
- Document findings and recommendations

The general tracking requirements have been surveyed and typical missions categorized. Two axis-tracking has been considered and impulse requirements investigated. Factors influencing tracker thermal response have been studied and thermal coating trends chosen. Several concepts for bimetal sun trackers have been developed and conceptual models fabricated. Preliminary tests were performed to "wring out" models prior to final testing. Fabrication of three models is complete, and a fourth is underway.

B. NOMENCLATURE

Symbol	
M	total mass
A	area
Q	heat
E	modulus of elasticity
H	angular momentum
ΔT	temperature drop
I	moment of inertia
L	coil active length
F	ASTM flexivity
a	acceleration
c	heat capacity
m	elemental mass
k	constant
t	thickness
q	heat flux
r	radius of curvature
v	linear velocity
w	coil element width
ϵ	emittance
α	solar absorptance
σ	Stephan-Boltzmann Constant
τ	time
ρ	density
ω	angular velocity

Subscript	
p	projected
t	total
i	initial
f	final
o	axis of rotation
c	coil

s	sink
h	high expansion element
l	low expansion element

SECTION II
TECHNICAL DISCUSSION

A. ANALYSIS OF DESIGN PARAMETERS

Investigation of design parameters affecting construction of conceptual test models has led to several specific areas of interest:

- A simple computer program was written and employed to note the effect of thermal coatings on coil temperature and cooling response.
- Specific bimetal elements were chosen for testing and analysis.
- A method of reducing axial coil motion to zero was devised and named "non-helical helix."
- Analysis was conducted to determine the allowable angular impulse input from the tracking system to the vehicle.

1. Thermal Cooling

Previous non-contractual tests were performed at LMSC on a reset-type bimetal tracking device. Those tests indicated that thermal response calculations using simplified coil thermal models were sufficiently accurate to obtain reasonable values of tracking rate and torque. Model tests were performed in a thermal vacuum chamber. It was found that analytical substitution of the helical coil by a cylinder of the same surface area provided an excellent correlation between thermal predicted and measured temperature. In this light, the simplified equations presented in Appendix A were used to study the effects of thermal coatings on coil response and equilibrium temperature.

A short computer program was written to study the effect of surface thermal properties on idealized bimetal coil cooling response. It was desired to obtain a basis for comparing thermal coatings so that bimetal coil response could be optimized. The result of this analysis is a determination of first-order thermal coating effects.

A matrix of cooling time was printed out for various values of α and ϵ. The matrix and a program listing are given in Appendix A. Values are calculated for a given coil thickness and temperature drop as a function of surface thermal properties. It was assumed that all radiation view factors were ideal and a zero sink was available.

Figure 1 is a plot of cooling time versus desired temperature drop for various values of surface properties. This particular plot is for a 0.020-inch thick coil but relates proportionally for a coil of any thickness. The trend is for minimum cooling times to be associated with high values of absorptance and low values of emittance. The high ratio of $\frac{\alpha}{\epsilon}$ is not necessarily the criterion but rather the specific values themselves, as is evident.

The identification of this trend is important in the design of devices in which the coil approaches its upper equilibrium temperature. A coil which provides work in a given temperature range (such as the stored energy device sensor coil), however, must be sized for its specific operating range. The fact still remains that best cooling response is obtained by operating the bimetal coil at a high rather than a lower temperature. In addition, at very low temperatures the coefficients of thermal expansion of bimetal components approach the same value. The flexivity* of the bimetal is thus reduced. The reduced flexivity necessitates a greater temperature change for the same amount of work and hence longer heating and cooling times.

2. Bimetal Element Properties

Models fabricated on this contract incorporate a high activity bimetal sandwich. "Truflex" 675-R (trade name for Texas Instrument Inc. bimetal series) is the highest flexivity bimetal material available. It consists of two alloys. The high-expansion

---

*Flexivity is the change of curvature of the longitudinal centerline of the specimen per unit temperature change for unit thickness or:

$$F = \frac{\left(\frac{1}{r_2} - \frac{1}{r_1}\right) t}{T_2 - T_1} \qquad (1)$$

where $\frac{1}{r_2}$ and $\frac{1}{r_1}$ are determined at T_2 and T_1 respectively.

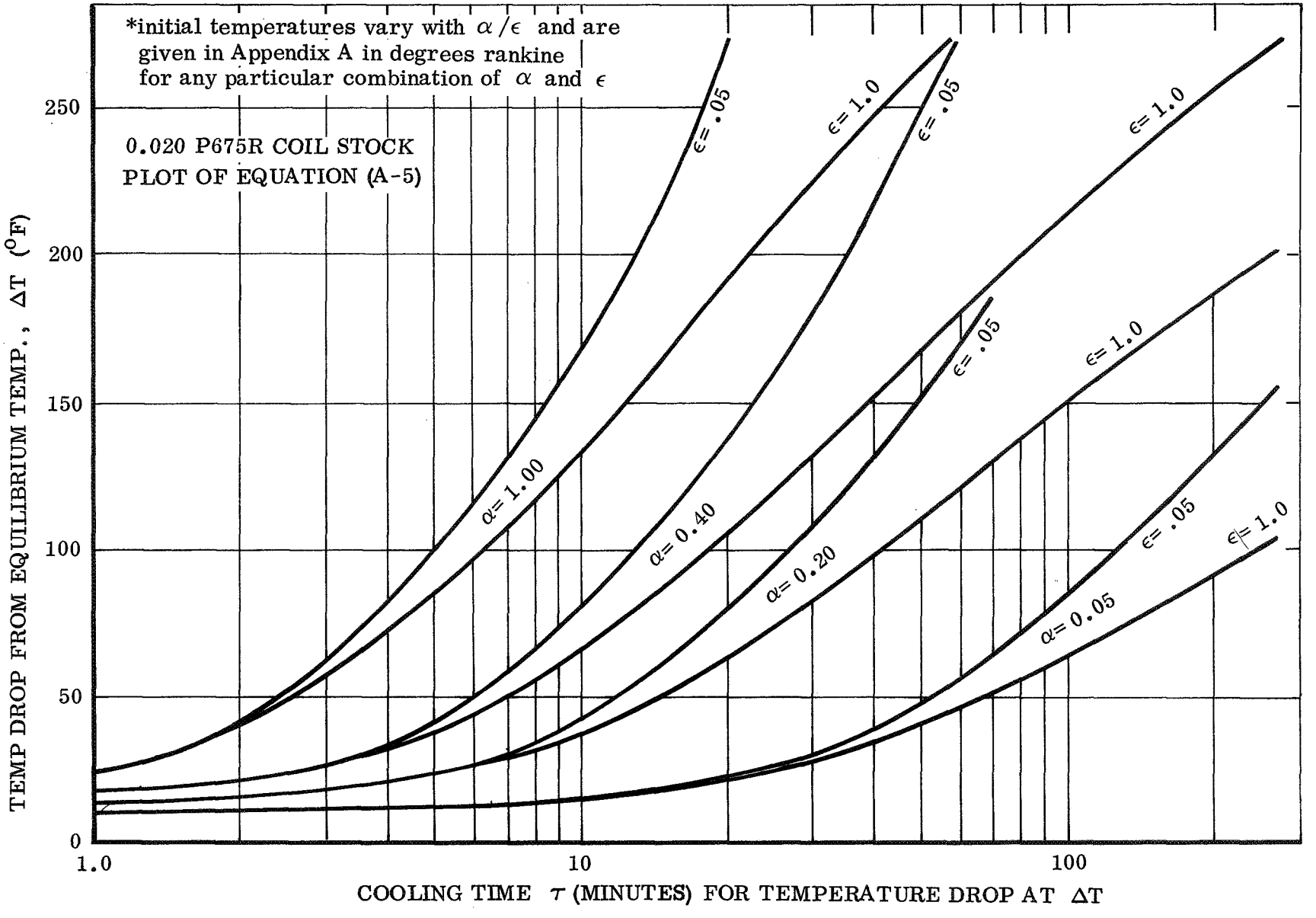

Fig. 1 Transient Coil Response

component, which makes up 55-percent of the total sandwich thickness, is 72 Mn-18 Cu-10 Ni. The other alloy is 36 Ni-64 Fe (Invar). The component thickness ratio is optimized to produce the maximum deflection possible according to the governing relation,

$$\frac{t_h}{t_l} = \left(\frac{E_l}{E_h}\right)^{1/2} \qquad (2)$$

The equivalent modulus of elasticity (E) of this material is 19.0×10^6 psi, and the density is 0.28 lb/in^3 with an electrical resitivity of 675 ohms/cmf at 75^{o}F. The P675-R is the most active bimetal and is also the most economical. Figure 2 shows a plot of ASTM flexivity for the element. The method of test for flexivity of thermostat metals is given in the 1961 Book of ASTM Standards, Part 3, (B106). Maximum sensitivity temperature range is 0^o to 400^{o}F, with a useful deflection temperature range of 100^o to 500^{o}F. Thermal heliotrope devices operate well within these limits. The maximum recommended temperature is 600^{o}F, but most uses are much below this value. Bimetal elements are very fatigue resistant, as witnessed by the heat riser valve in most any automobile engine. In addition, low temperature liquid nitrogen dip tests were performed on a sample coil. Twenty cycles from 75^{o}F to LN temperature produced no damage or permanent deformation.

Figure 2 also shows a flexivity curve for PJ bimetal material. Although the flexivity is low, the material is essentially non-magnetic and fails to show any induced magnetism with magnetizing forces of up to 250 oersteds. Its component materials are 72 Mn-18 Cu-10 Ni for the high-expansion element and 1.5 Si-0.3 Mn-98.2 Cu (Silicon Bronze) for the low-expansion element. Equivalent modulus of elasticity is 17×10^6 psi, which is the same as the component alloys, and density is 0.30 lb/in^3. The P675-R elements used on the conceptual models were given a 50-percent physical reduction in manufacture to obtain the desired spring properties. The range of vickers hardness is 190-240 for the high-expansion component and 210-260 for the low-expansion element. Also, the material was chemically etched (designated LES etch by the manufacturer) to increase emissive properties and clean surface micropores of oils and impurities obtained in the manufacturing rolling operation.

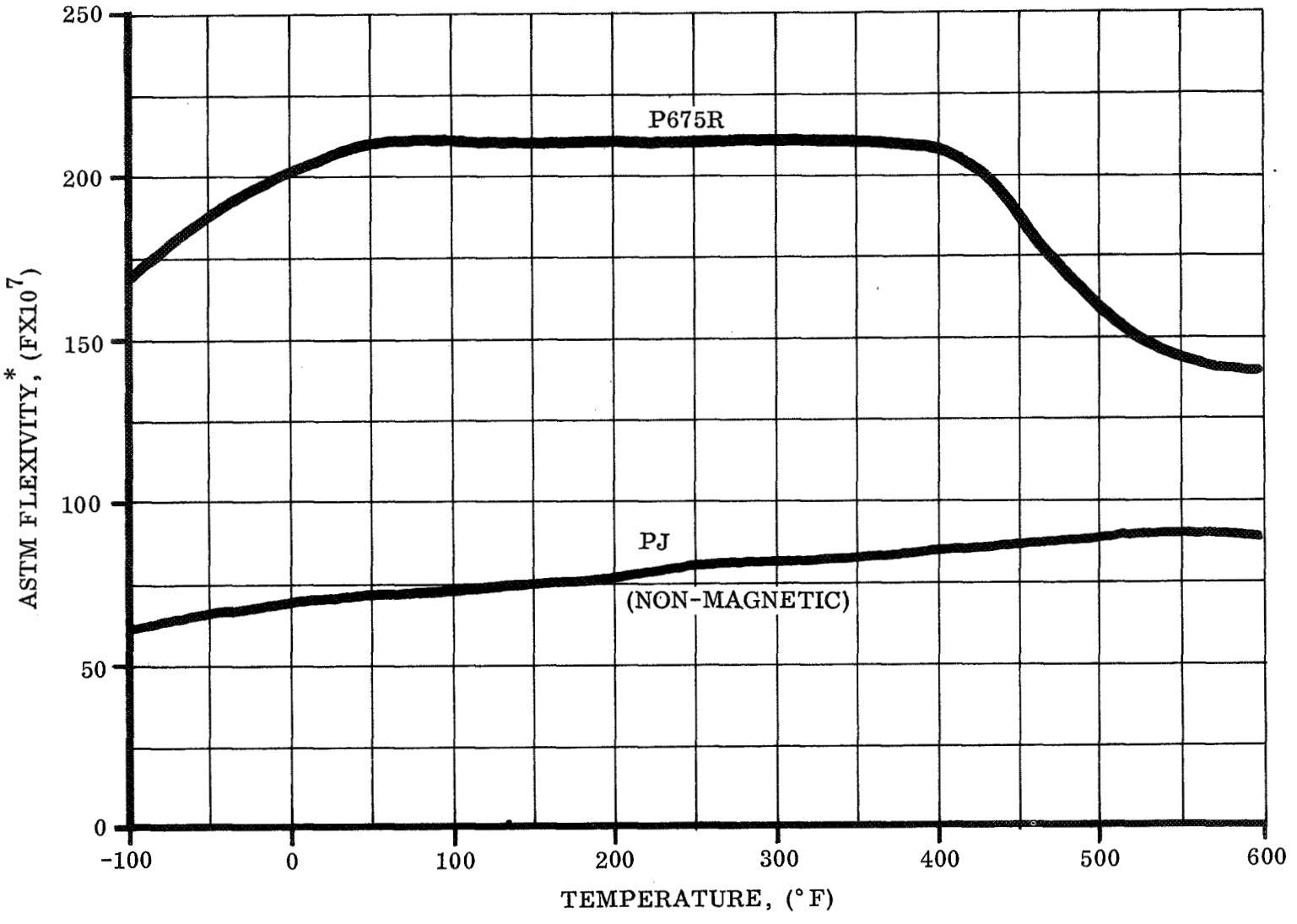

*ASTM STANDARDS, 1961, PART 3 (B106)

Fig. 2 Bimetal Flexivity

After helical forming, but prior to thermal coating and model installation, the bimetal material was given a stabilizing heat treatment for 60 minutes at $450^{o}F$. This relaxes forming stresses so that no permanent deformation occurs during model operation.

As presented in the first quarterly report, the following relations apply to helical bimetal coils:

$$\text{restrained torque} = 1.55\ E\ F\ (\Delta T)\ w\ t^2 \tag{3}$$

$$\text{mass} = \rho w t\ L \tag{4}$$

$$\text{unrestrained deflection} = \frac{67F\ (\Delta T)\ L}{t} \tag{5}$$

The constants contain the units required to balance the equations dimensionally so that the torque is given in in.-oz, linear measurements in inches, and angular displacement in degrees arc.

It may be seen from these equations that

$$\left\{\frac{\text{restrained torque}}{\text{mass per degree of unrestrained deflection}}\right\} = (\text{constant})\ x\ (\Delta T)^2 \tag{6}$$

For any given ΔT (function of thermal coatings and shade elements), the restrained torque varies directly with the "mass per degree of unrestrained deflection". However, it is desirable to have large values of torque and low values of mass. The related variable here is $(\Delta T)^2$; thus, ΔT should be maximized in the design of helical elements. Note that this ΔT is the maximum potential ΔT from upper equilibrium temperature to lower temperature (a function of shade time and configuration). It is not the actual operating ΔT, which is somewhat smaller.

Variation of restrained torque with mass is shown in Fig. 3. This figure is relevant for sensor-type elements where angular displacement is small. The relative mass is for a coil of unit length. It may be seen that for a given required torque several coil configurations are possible. For example, for a required sensor torque of 12.3 in.-oz

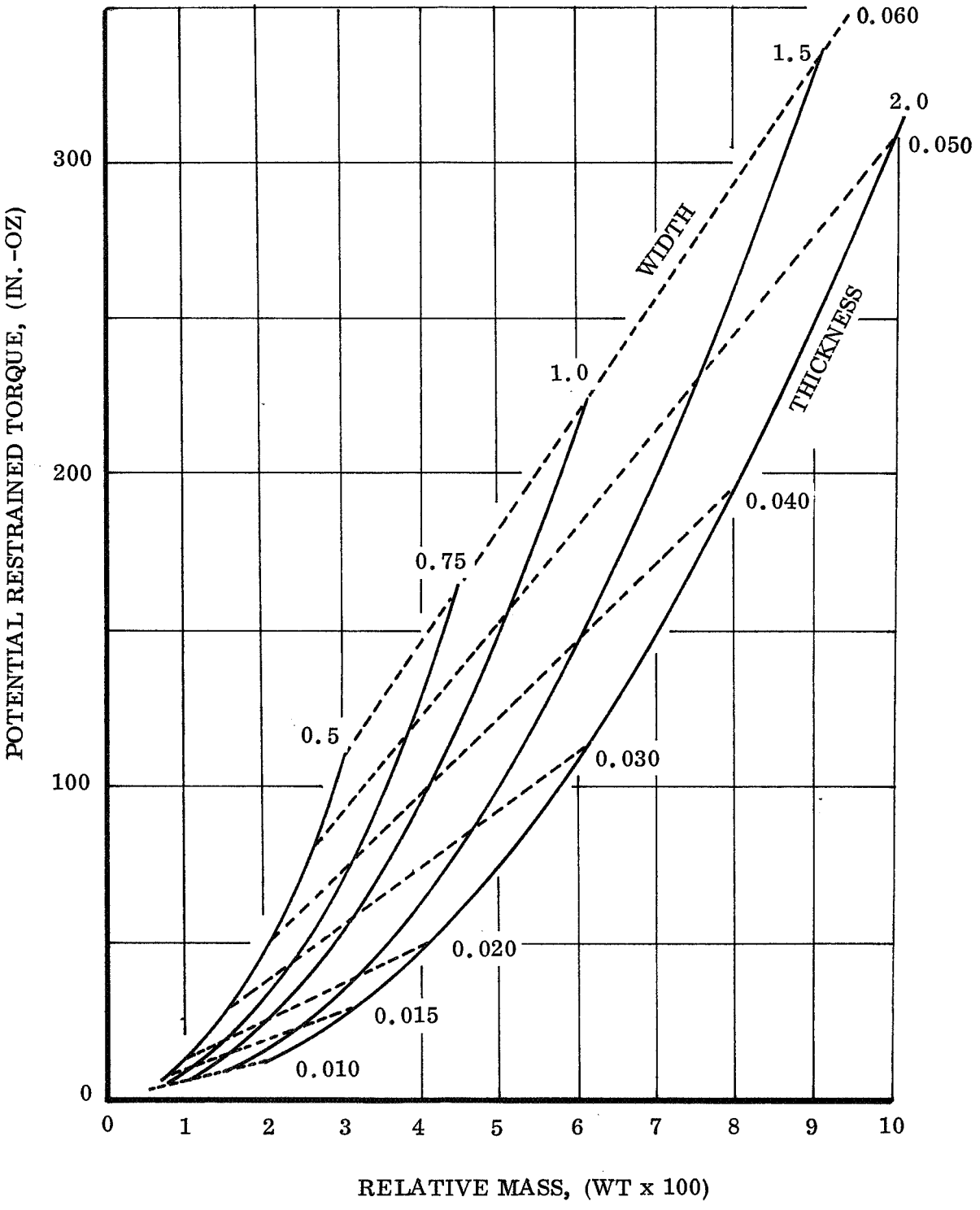

Fig. 3 Sensor Coil Torque Potential for 100°F ΔT (P675-R Bimetal Material)

coil choices include a 0.020-inch thick 0.5-inch thick 0.5-inch wide element and a 0.015-inch thick element about 0.9-inches wide. The narrower element gives the lowest mass; however, thermal response considerations would probably dictate use of the thinner element. Since the total coil mass is relatively small, the thermal considerations predominate.

3. Thermal Coatings

A selective acidic oxidation of the bimetal components (a Lockheed-developed oxidation process) allowed formation of a thin oxide layer with predictable thermal properties. The layer is dark in appearance and controlled by a timed soak in the oxidizing medium, followed by immediate flush. Dip times of several minutes produced extremely durable surface layers. During the process, absorptance increases more rapdily than emittance; thus, by relating dip time to pre-tested sample properties, a given ratio may be obtained. Typical absorptance values obtained with this process were 0.88 to 0.93 with corresponding emittance values of 0.30 to 0.65. This coating treatment was used on both coils of the stored energy device. No degradation of surface properties was noticed before, during, or after preliminary testing. The metallic coating has the advantage of being thin and thermally conductive, thus preventing a significant thermal resistance between the element and environmental sink.

The alpha adjuster coils were coated with 3M black velvet, number 161-C10. This coating has an absorptance approaching 0.95 and an emittance of over 0.90. It is applied over MIL-P-8585A zinc chromate primer and baked dry. The coating provides an upper equilibrium temperature of less than $100^{o}F$ but is sufficient for seasonal adjustment devices. These coils were not treated with the LES etch (a Texas Instrument etch process), but no coating failure occurred. The slotted shade mechanism on the stored energy tracker was coated with a low-absorptance, high-emittance coating to provide cool surface temperatures, good temperatures, and good radiative cooling of the sensor coil. White Thermatrol (2A-100) silicone paint was used which has typical absorptance and emittance values of 0.16 and 0.95, respectively. This is a flight-proven material which is highly resistant to ultraviolet, low-energy electron and thermal

cycling degradation. It has an elastromeric surface, which is easily repaired in case of damage. The surface may pick up a slight electrostatic charge in ground handling, which is sufficient to attract dust particles. Cleaning, however, is easy with Freon TWD and distilled watter. Freon TWD is a mixture of Freon TF (Dupont) and a Dupont detergent (TWD-602). The mixture will remove water soluble salts as well as oils.

4. Non-Helical Helix

In devices incorporating a planar shading arrangement for shading a coil (like the feedback shade used on continuous devices other than the stored energy tracker) it is desirable to minimize the necessary angle of shade rotation between a fully illuminated and fully shaded mode. This angle, called the shade angle (Fig. 4a) is a function of coil diameter and shade distance from the coil $\left(\theta = 2 \tan^{-1} \frac{\text{coil radius}}{\text{distance from shade to coil}}\right)$. Coil winding diameter can be reduced by minimizing angle θ without having an excessively long shade-coil distance. A small diameter helical coil, however, is not practical when using wide coil stock (a necessity for torque requirements). Winding the small diameter coil produces a high helix angle (Fig. 4b). With a high helix angle, considerable torque capability is lost due to bimetal action, causing motion along the winding axis instead of around it. To avoid this situation, a zero angle "helical" coil may be constructed, as shown in Fig. 4c. Any width bimetal stock may be formed into small diameter segments and fastened together, as shown. Thus, it is possible to wind small diameter coils of relatively large width bimetal stock without obtaining undesirable axial element expansion.

Where pure linear axial motion is desired, coils may be wound in a double helix configuration. Considerable force is available for small deflections with these coils. Area effectivity for radiative heat transfer is about 15-percent lower than for a pure helix; however, the linear force is greater. This type of coil may have application as a sensor in the triggering motion of springmotor or shade devices.

5. Tracking Impulse and Torque Requirements

a. Angular Impulse. A typical angular momentum requirement for a very accurately pointing synchronous vehicle is in the order of 2.5×10^{-3} ft-lb-sec. That is, the

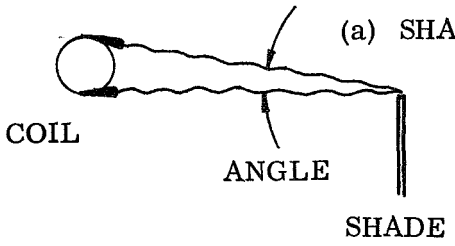

(b) CLOSED HELIX GEOMETRY

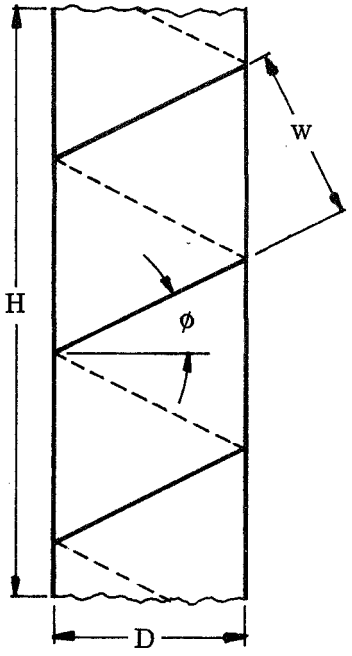

N = NUMBER OF COILS
L = ACTIVE LENGTH
w = STRIP WIDTH
D = COIL DIAMETER
H = SOLID HEIGHT
ϕ = HELIX ANGLE

$$\phi = \mathrm{Sin}^{-1} \frac{w}{2D}$$

$$N = \frac{H}{2D \tan \phi}$$

$$H = \frac{w L}{\pi D}$$

(c) ZERO ANGLE HELIX

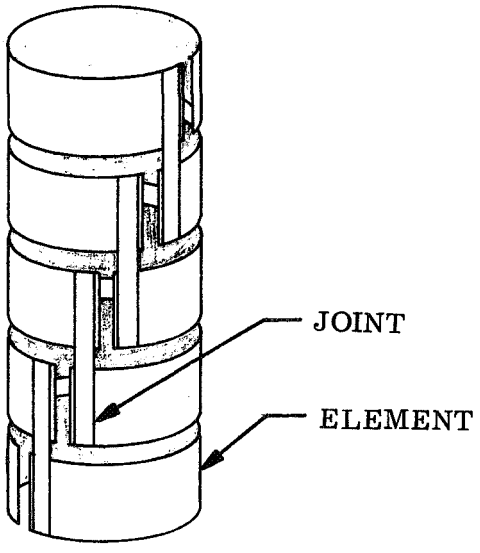

Fig. 4 Helical Bimetal Coils

solar array tracking mechanism may impart a momentum impulse to the vehicle of this amount. Translated into oz-in. units, the value is 0.48 oz-in.-sec or about 0.5 oz-in.-sec. The total angular momentum of a body is given by

$$H_o = \Sigma mR^2\omega + \Sigma mv_{oy}x - \Sigma mv_{ox}y \tag{7}$$

or

$$H_o = I_o\omega + \bar{x}mv_{oy} - \bar{y}mv_{ox}. \tag{8}$$

The axis notation is explained in Appendix B.

When the axis of rotation is fixed (pure rotation), this expression is reduced to

$$H_o = I_o\omega \tag{9}$$

The relation between the angular momentum of a body and the applied moments is obtained from the rotational equation of motion. The sum of the moments of all forces about o is

$$\Sigma M_o = I_o\alpha = I_o\frac{d\omega}{d\tau} \tag{10}$$

$$\Sigma M_o = \frac{d}{d\tau}(I_o\omega) \tag{11}$$

This means that the resultant moment about the fixed axis of pure rotation equals the time rate of change of angular momentum about the respective axis. This relation holds during the entire time of motion and may be integrated to give

$$\int M_o\, d\tau = I_o\omega - I_o\omega_o = I_o(\Delta\omega) \tag{12}$$

Thus, the total angular impulse equals the corresponding net change in angular momentum. A similar situation holds true for rotation about an axis through the center of mass so that

$$\text{impulse} = I(\Delta\omega) \quad (\text{ft-lb-sec}^2) \quad \frac{\text{rad}}{\text{sec}} = \text{ft-lb-sec} \tag{13}$$

(where I is the moment of inertia about the center of mass)
or alternatively for constant Γ application,

$$\text{impulse} = \Gamma(\Delta\tau) \tag{14}$$

Conservation of momentum requires that when there are no externally applied moments on a system about a fixed axis (gas jets, etc.), the angular momentum of each part may change, but the total angular momentum of the system about this axis is conserved. Thus, every change in solar array momentum is transmitted to the vehicle and must be absorbed by the attitude control system. For the case in point, with a low allowable impulse input the permissible change in angular rate (for constant I) is very low. For example, a pair of $10\,ft^2$ solar panels at $1.1\ lb/ft^2$ have an $I = 0.5$ slug-ft^2. An allowable impulse of 2.5×10^{-3} ft-lb-sec means that the maximum rotational speed from initial rest is about 17.2 deg/min.

This rate is more than adequate for tracking in the fastest possible orbit, but individual increments of incremental tracking devices may naturally occur at a higher rate. It may be seen then that incremental tracking devices may require governing to prevent excessive impulse input to the vehicle. This governing may be accomplished by means of a mechanical device or by limiting the torque capability of the tracker itself. However, it appears difficult to accurately control torque to such a low level while still having enough to compensate for friction which cannot be accurately predicted over the vehicle lifetime.

The preceding discussion has addressed itself to vehicles with extremely low impulse limitations. Many programs do not have such tight requirements, and incremental tracking is applicable. However, for those programs that do require non-incremental tracking motion a two-coil continuous tracker has been devised and is discussed further in this report.

b. Torque. As discussed in the previous quarterly report, actual tracking torque required to overcome the solar array inertia is extremely small. The determining factor in torque requirements, then, is friction within the system. This is especially the case of continuous trackers which require some type of slip ring rotary power transfer joint. Rotary joint friction was computed for a test case to determine the order of magnitude of frictional torque. Consideration was given to a slip ring unit with primary and capsule bearings. Bearing preloads determined frictional torque. Power brush area, number, and loading determined the drag for the slip ring system. Signal brush torque was also considered. The total frictional torque for a 6-power ring, 10-signal ring system applicable to a tracking solar array vehicle is about 16 in.-oz. This value is well within the range of the thermal heliotrope devices considered.

B. CONCEPTS AND DEVICES

In this section the basic mode of operation of specific concepts is discussed. In addition, construction details of models fabricated to date are presented, and photographs of disassembled hardware are included.

1. Operation modes of Concepts

a. Planetary Shade Tracker. The planetary shade tracker, shown in Figs. 5 and 6, derives its name from the technique whereby the coil shade moves with respect to the coil. The shade is mounted on a rotating shaft which is coupled to the coil fixed end or vehicle via a small gear. The rate or times at which the shade alternately shades or allows illumination of the bimetal helical coil per 360^{o} of rotation is a function of the diameters of the fixed wheel or gear and the planetary gear. It is desirable to

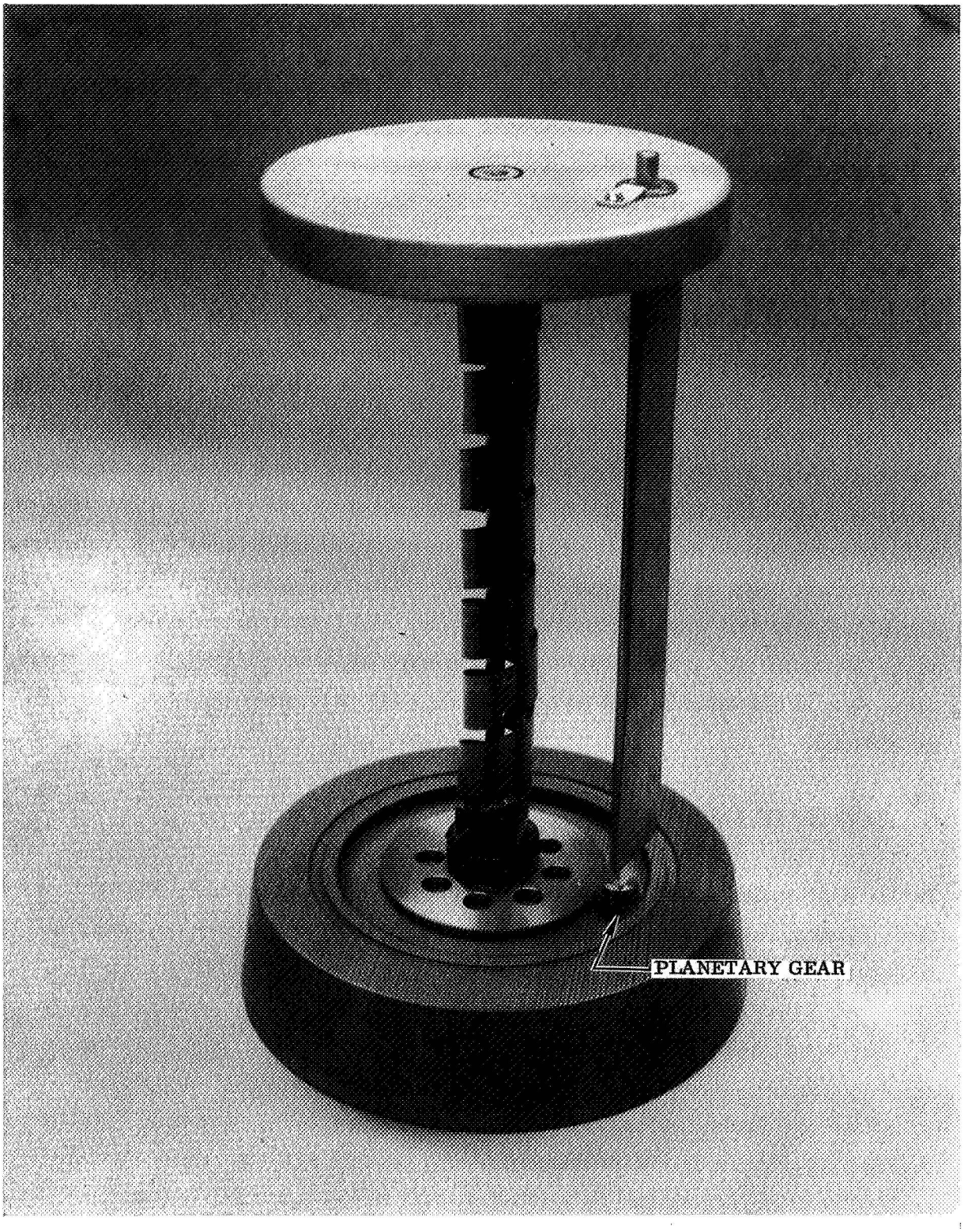

Fig. 5 Planetary Shade Device (Desk Top Model)

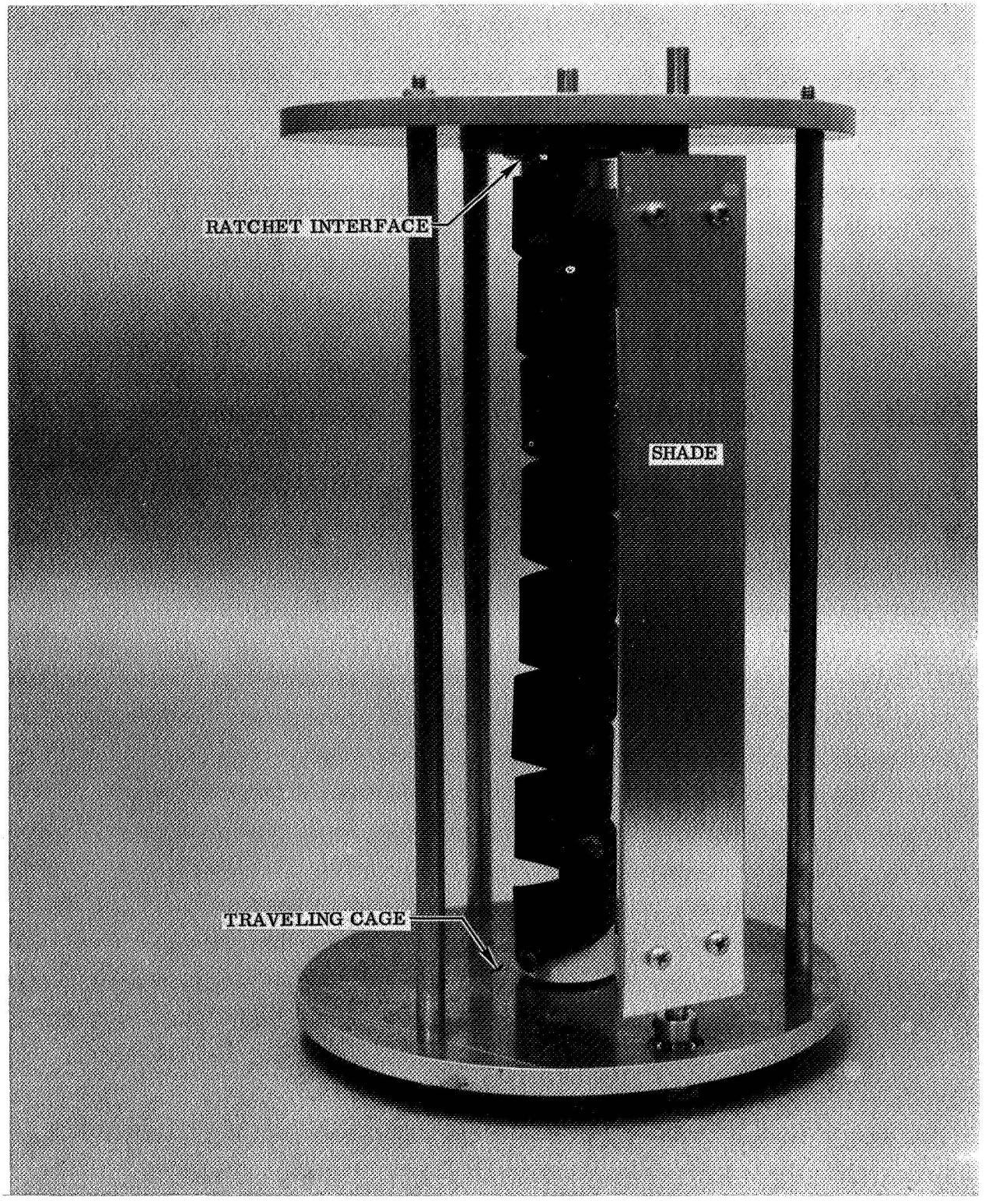

Fig. 6 Planetary Shade Device (Test Model)

have a large fixed gear diameter and a small planetary gear diameter to effect rapid full shading as a function of orbital rate, allowing the coil to reset so that continuous tracking can be achieved. Coil reset occurs in that the coil is ratchet-coupled to the shade assembly cage at one end. As the coil is illuminated and heated, the coil free end rotates unidirectionally at a rate faster than the orbital rate. This causes the shade cage assembly to rotate bringing the shade, which is coplanar with the array, around so that its face is directly between the sun's rays and the coil. Within the shade, reset occurs. Continued vehicle orbiting, or apparent sun displacement, again causes illumination upon the coil. This illumination is expanded because of the contra-rotation of the planetary shade. Coil rotation results and the cycle is repeated.

The planetary shade tracker concept is closely related to the reset-type tracker. If the feedback shade rotated, it would be similar to the planetary shade. Also, if the planetary shade tracker coil were fixed at both ends, unable to ratchet and reset, the unit would be a reset-type tracker rather than a continuous tracker.

b. Seasonal Adjuster. The function of the seasonal adjuster-type tracker, shown in Figs. 7 through 9, is to make incremental position adjustements of a solar array, bi-directionally to a more optimum incidence to the solar vector. For low earth polar orbit, this adjustment would occur as the vehicle passes through the ecliptic plane at a frequency dependent upon the daily progression or retrogression in the orbit plane angle. Rotation or adjustment of the array is effected by illumination of a CW or CCW coil causing it to expand, walk an engagement gear into a fixed sun gear, and rotate the drive assembly and the array. As the coil cools, it contra-rotates and moves the engagement gear away from the sun gear. Thus, the non-working or non-illuminated coil is always disengaged except when it has a specific correction function to perform. When the assembly is properly oriented, both coils are at rest and disengaged.

This type of tracker could be applied to a synchronous equatorial array to adjust the array within the $\pm 23.5^{\circ}$ seasonal change from winter solstice to summer solstice. This would keep the array in the more optimum equinox position.

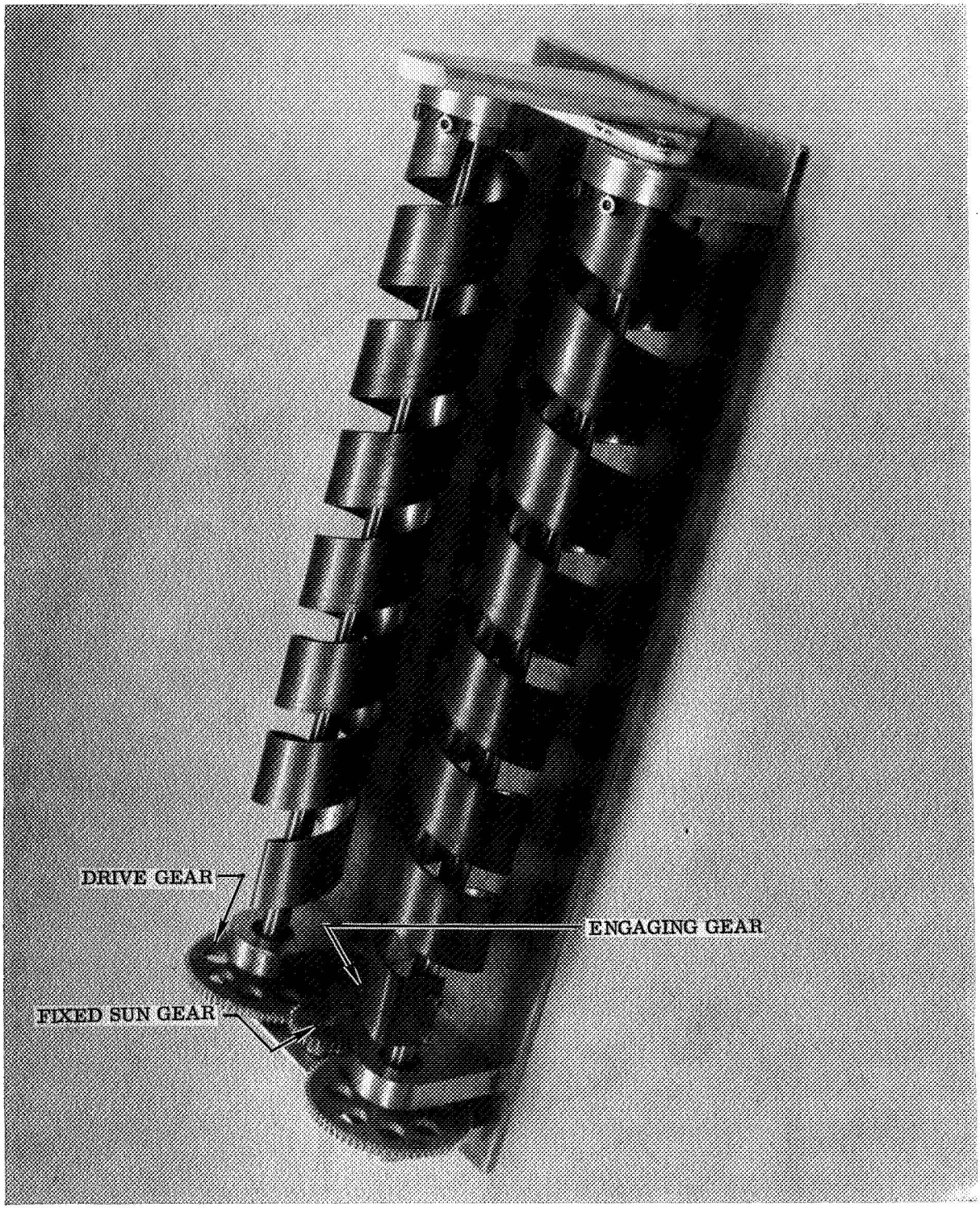

Fig. 7 Seasonal Adjuster During Fabrication

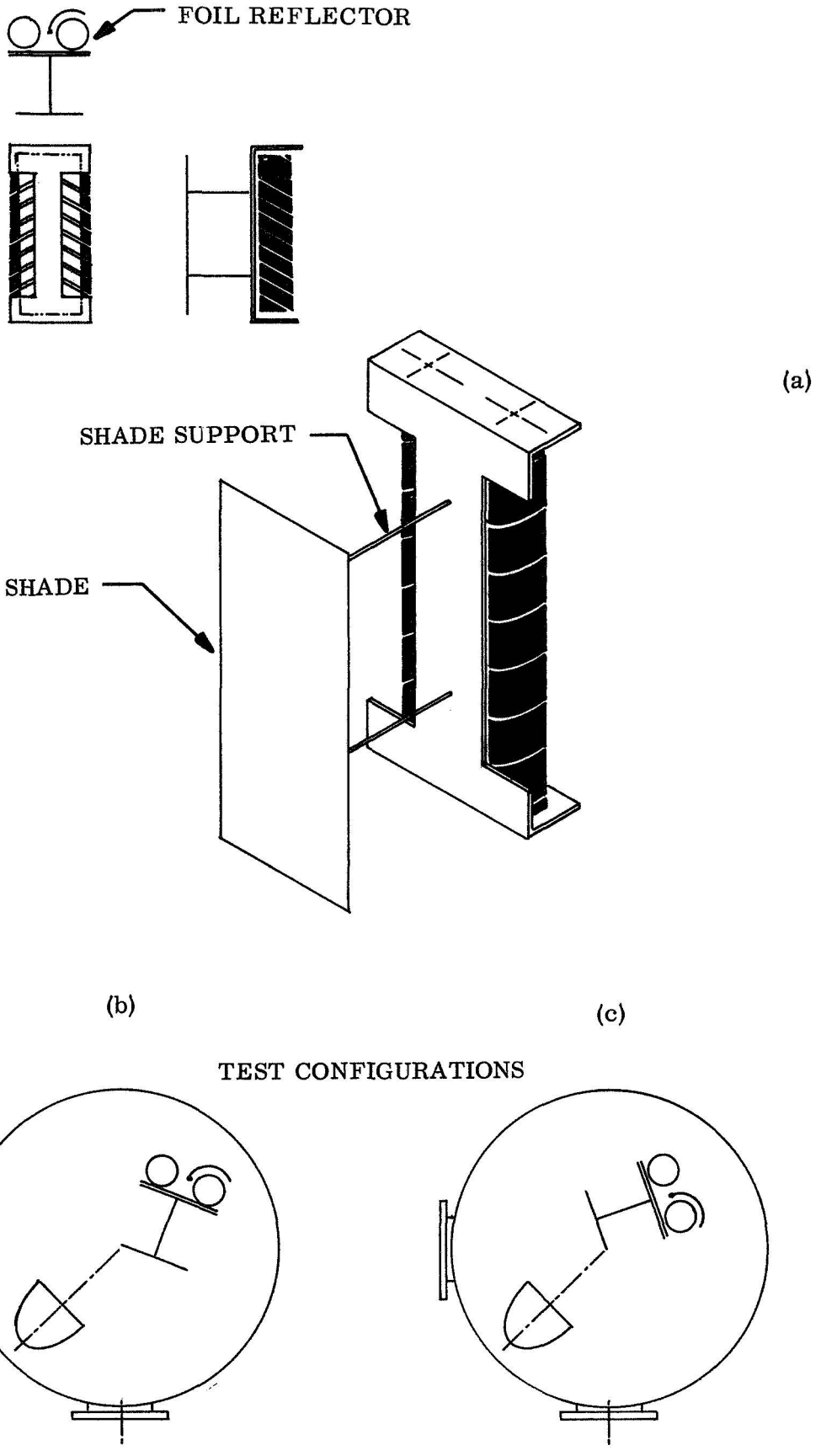

Fig. 8 Seasonal Adjuster

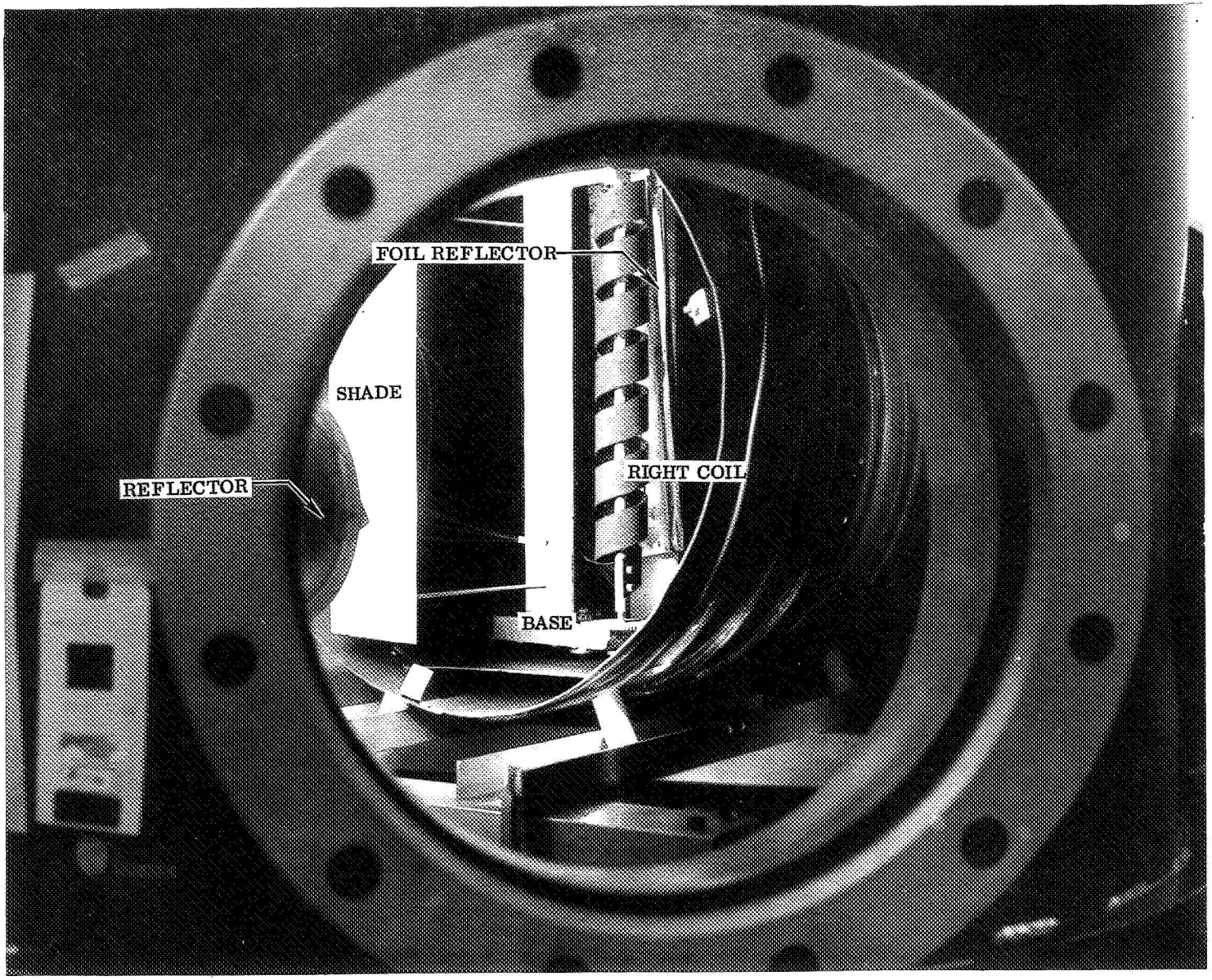

Fig. 9 Seasonal Adjuster Under Test

There are also a variety of lunar orbiting and lunar surface solar photovoltaic power applications where a bi-directional incremental adjustment tracker of the Seasonal Adjuster type could be used to great advantage. The inherent simplicity, reliability, and unlimited life would make the device ideal for remote unattended lunar surface photovoltaic power systems.

c. Stored Energy Tracker. To optimize both sensing and motor functions of a bimetal tracker, it becomes necessary to incorporate two coil elements. One element is designed to be highly responsive to thermal changes for the sensing function. This element will necessarily be thin with low torque capability. The other coil is thicker, with considerable torque capability and associated low thermal response. The coils are shown in Fig. 10. In operation, the higher torque motor coil is thermal-cycled via static shades as the vehicle traverses its orbit path. The cycling produces rotary motion that winds a constant torque spring. Thus, throughout the vehicle orbit there is always a source of stored energy available. The low-torque-sensing element reacts to illumination (heating) and trips an escapement to provide an increment of tracking motion. A concentric slotted shade system allows orientation of the solar panel from any initial misorientation and a lock-on capability for routine tracking. The lock-on function is provided by a non-slotted portion in the shade system that will prevent the sensor coil from being illuminated (and thus tripping the escapement) when the solar panel is normal to the sun. Step-by-step explanations of the energy storage and tracking modes are given in the first quarterly report of this contract*.

d. Two-Coil Continuous Heliotrope. Requirements for solar array tracking systems that impart very low angular impulses to the vehicle have lead to a continuously tracking heliotrope concept. Several synchronous and intermediate altitude spacecraft require precise antenna pointing and stabilized vehicle orientation. Incremental solar array sun tracking in these cases may be less desirable than a continuously tracking system.

*Passive Solar Array Orientation System, Second Quarterly Report, NAS 5-11637, 23 Dec 1968 – 23 Mar 1969, pg 45

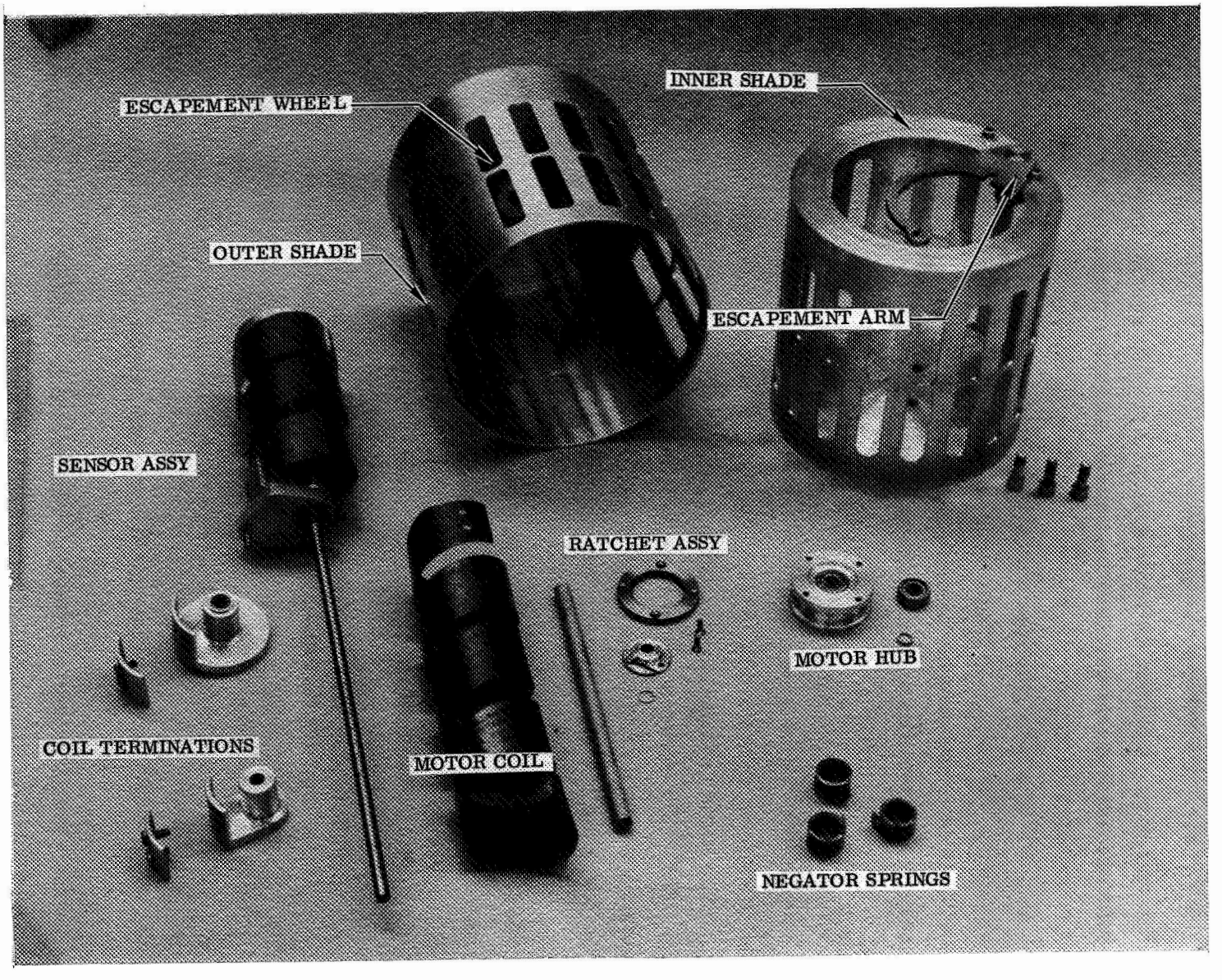

Fig. 10 Stored Energy Device Components

A double coil device has been devised which will provide smooth continuous tracking. Two coils are used so that they may be made of sufficient thickness to provide adequate torque capability. A high torque coil cools slowly in the reset mode, so two units are used. One coil at a time provides tracking motion while the other is cooling from a previous cycle. The device is shown schematically in Fig. 11(a). Both coils are fastened at their outboard ends to the drive gear, which rotates about the mounting shaft on bearings. A reversing gear on each drive gear provides the correct directional sense to the pawl carrier gears. Each of these gears carries a simple spring-loaded pawl which rides against a ratchet wheel. The ratchet wheel has only one tooth in order to assure positive array synchronization with the tracking coils. A sketch of the pawl/ratchet system is shown in Fig. 11(b). The ratchet wheel is mounted to the array drive shaft, which turns relative to the vehicle interface. The shading arrangement is shown in Fig. 12(a). The static shade is fixed relative to the vehicle, while the feedback shades (one for each coil) rotate with the coil drive gears. The feedback shades are arbitrarily in the hot coil position. The attachment interface is illustrated in Fig. 11(b).

Operation mode of the device is shown in Fig. 12(b) and a brief explanation follows (F indicates the front coil and B is the back coil):

1. Coil F is hot and has finished its tracking cycle. It has reached a mechanical stop and no further rotation will occur. Coil B is cold against a stop and ready to take over the tracking action.
2. Coil F is becoming shaded by the static shade while coil B is becoming illuminated. Tracking by coil B has been initiated.
3. Tracking is being controlled entirely by coil B. Coil F begins its reset cooling cycle.
6. Coil B is hot and has finished tracking. The transition between coil B and coil F beings.
7. Coil F is tracking while coil B cools and resets.

In the transfer zones proper alignment of shades and mechanical stops will assure a smooth transition between coils. There is no incremental motion or anap action as transfer occurs and thus minimum impulse, transmitted to the spacecraft. For synchronous application each coil would have up to twelve hours for reset cooling. This would allow a drive coil to be sized for more than enough torque to provide tracking for most any sized array. It should be noted that the figures of the continuous tracker are conceptual sketches. For model fabrication the shade system and drives will be streamlined.

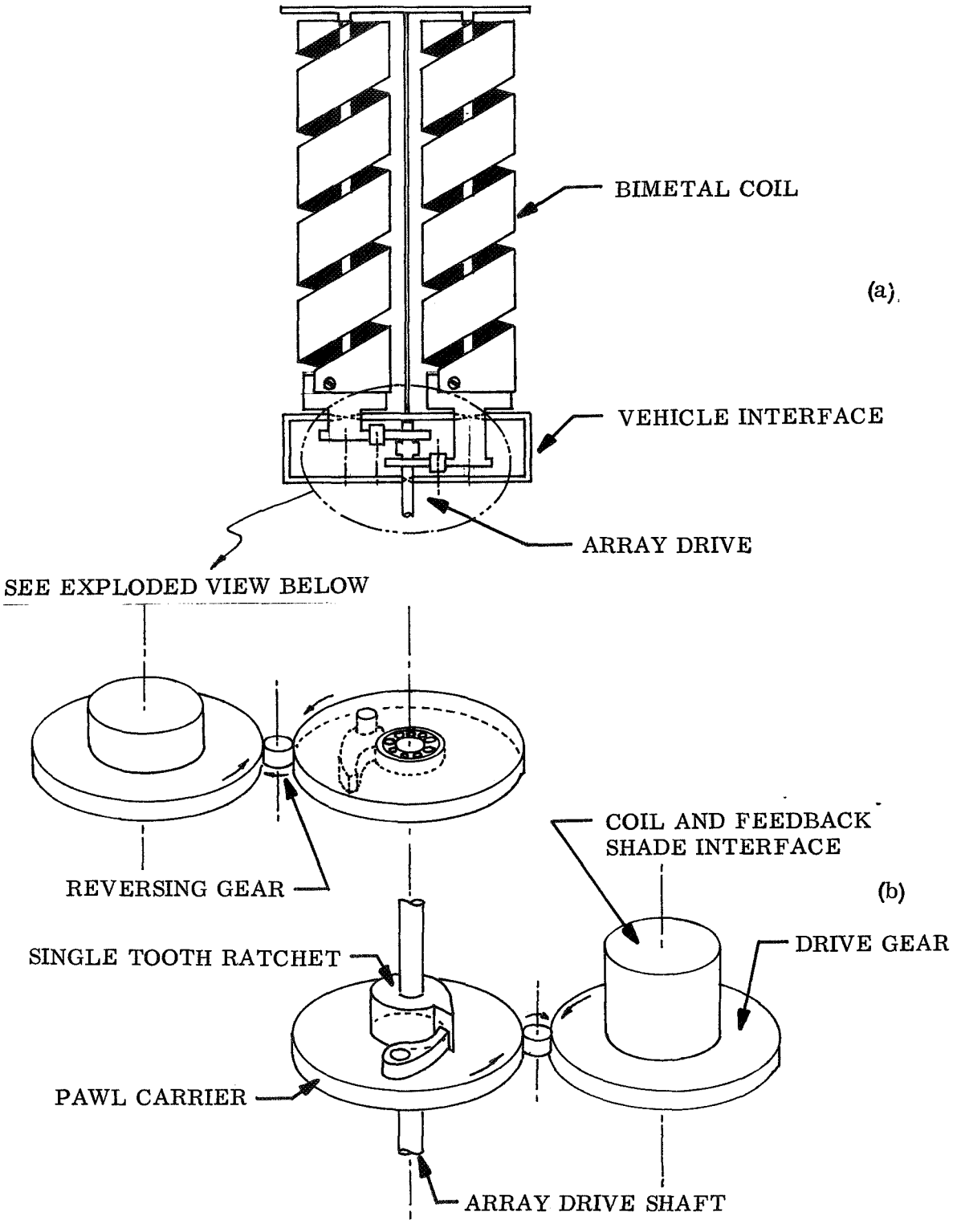

Fig. 11 Two Coil Continuous Tracker

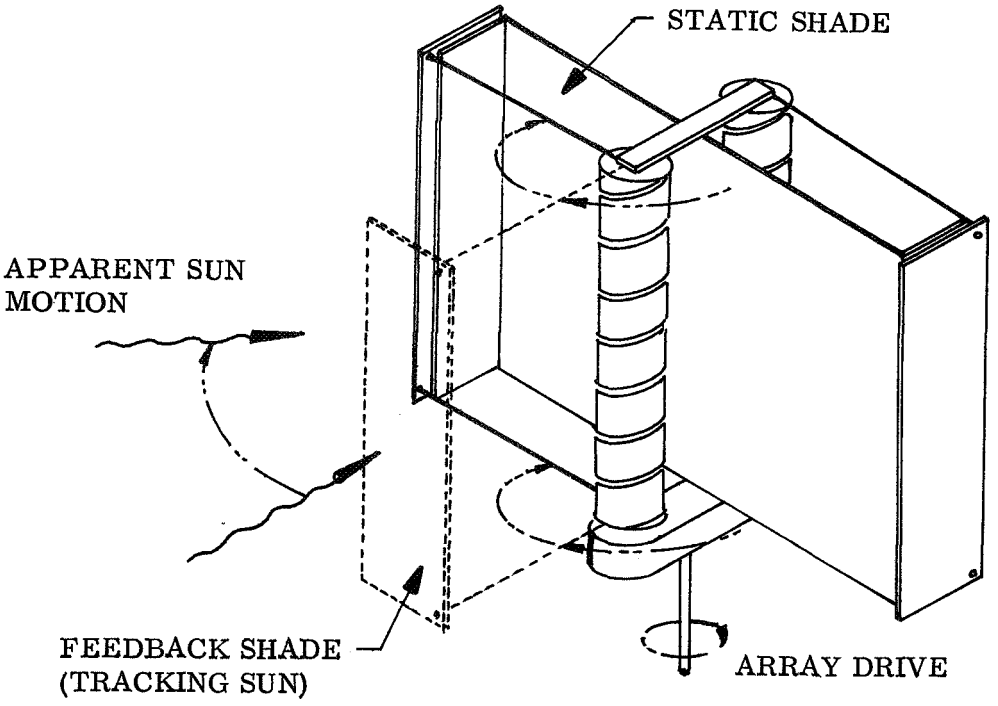

(a)

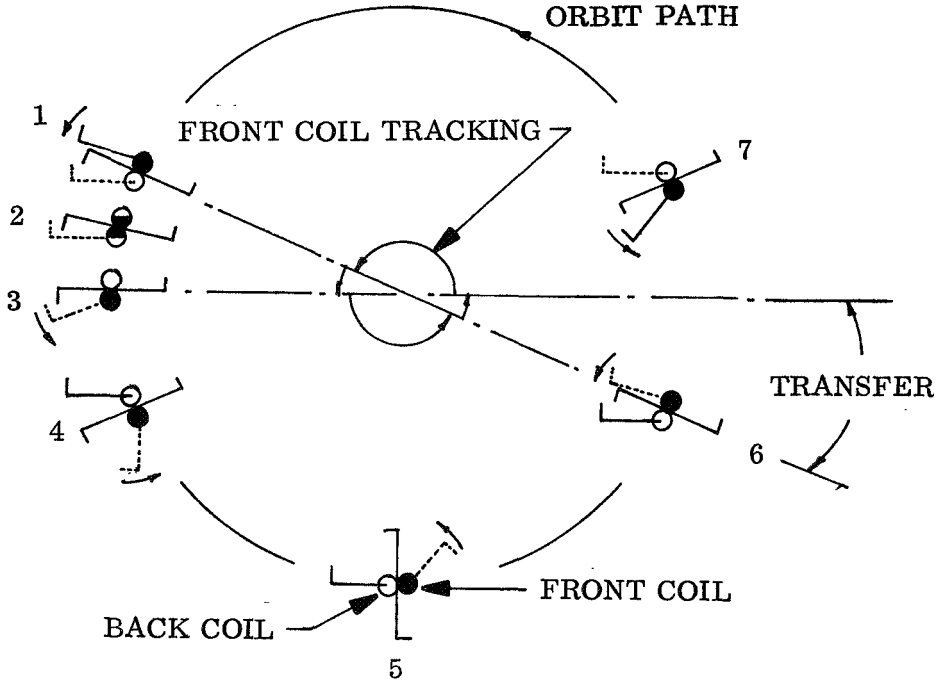

(b)

Fig. 12 Continuous Tracker Concept Configuration

2. Construction of Conceptual Models

During the reporting period initial fabrication has been completed on three thermal heliotrope test models, and a fourth model is nearing completion. The planetary shade device, seasonal adjuster, and stored energy device are complete. Preliminary testing was done to "tune" the models and determine suggested modifications. The testing indicated that a thicker coil was needed to provide smooth tracking motion with the planetary shade device. Slight shade modifications are necessary on the seasonal adjuster to prevent illumination of both coils simultaneously. The stored energy device needs no further work. The following paragraphs describe the physical features of the three completed models. It should be noted that the models are designed for concept proof test and do not reflect flight hardware configurations.

a. Planetary Shade Tracker. To examine the feasibility and function of the Planetary Shade Tracker concept, a desk top model was fabricated. This model is illustrated in Fig. 5. The base and top of the model were constructed of wood, redwood and pine, respectively. The base was indented to provide a raceway where the planetary gear could rotate around the major rotational axis, as driven by the larger ratchet coupled gear. The bimetal helix was formed by hand around a 5/8-in. diameter dowel using a 0.15-in. thick P675-R. The helix was fixed on its upper end to a 1/4-in. steel rod that projected from the base. As the helix was heated, its lower end was free to rotate, engage the lower drive gear, and effect rotation of the planetary shade around to a point where the helix was shaded. Operation of the desk top model was adequate for demonstrating the concept and function of a Planetary Shade Tracker.

Next, a test model of the tracker was fabricated. As a result of thermal analyses, the outside surface of the helix was coated with 3M black velvet coating No. 101-C10 after priming with MIL-P-8585A yellow zinc chromate (no application specification). This coating has an $\frac{\alpha}{\epsilon}$ ratio of nearly unity, with high values (0.8) of both absorptance and emittance. The helix assembly is shown in Fig. 6, with its terminations isolated from the mounting structure by glass tape to minimize the thermal losses by conduction. The test model was comprised primarily of a three-strut cage assembly which contained planetary shade bearings at its upper and lower plates. The cage also

contained an internal gear underneath the top plate which provided a ratchet coupling interface for the bearing-supported helix free end termination. The cage assembly rotated as driven via the helix ratchet coupling when illumination-induced helix heating occurred. The cage rested and rotated on a stationary or fixed sun gear which is barely discernible in the shadow below the lower cage plate. The planetary shade contra-rotated with major cage rotation via the small planetary gear engagement with the sun gear. The planetary and sun gears selected were of the Precision Instrument Corporation types. The gears used were, respectively, part numbers J25-320 and G45-30, the largest and smallest stock sizes available for the sun and planetary to effect the maximum shade cycles per assembly revolution. Flight hardware configurations could utilize specially designed gears to maximize the gear ratios and achieve more shade cycles per revolution.

b. Seasonal Adjuster. Figure 7 is a photograph of the seasonal adjuster midway through fabrication. Shown are the two 0.060 stock P675-R bimetal coils; one is reverse wound to provide rotation in both directions. Both coils are fixed to terminations at one end, and their free ends are mounted to shafts which rotate in ball bearings. Drive gears are fastened to the ends of these shafts. A sun gear is positioned between the drive gears and is considered hard-mounted to the vehicle. Figure 7 shows the relationship between the sun and drive gears. Two engaging gears ride in slots to provide a train between the sun and a drive gear during the tracking mode. Coil heating turns the drive gear. This gear pulls in the engaging gear, and the assembly tracks. Cooling of the coil backs out the engaging gear without affecting array position. An adjustable aluminum shade is mounted to the device, as illustrated in Fig. 8(a). The shade may also be seen in the photo of the test setup, Fig. 9. Coil rods ride in ball bearings sonic cleaned in MEK and alcohol. The unit is mounted in a saddle frame to facilitate testing.

c. Stored Energy Device. The stored energy device is shown in Fig. 13 prior to the application of thermal coatings. Both motor and sensor coils are wound from "Trueflex" P675-R stock with the low expansion alloy (Invar) on the outside. The 0.020-inch stock motor coil is hard-mounted to the main shaft at the upper end and free to turn the ratchet assembly at the lower end. Small curved plates provide coil support at both terminations (also shown in Fig. 10). The base coil termination carries a ratchet pawl as shown

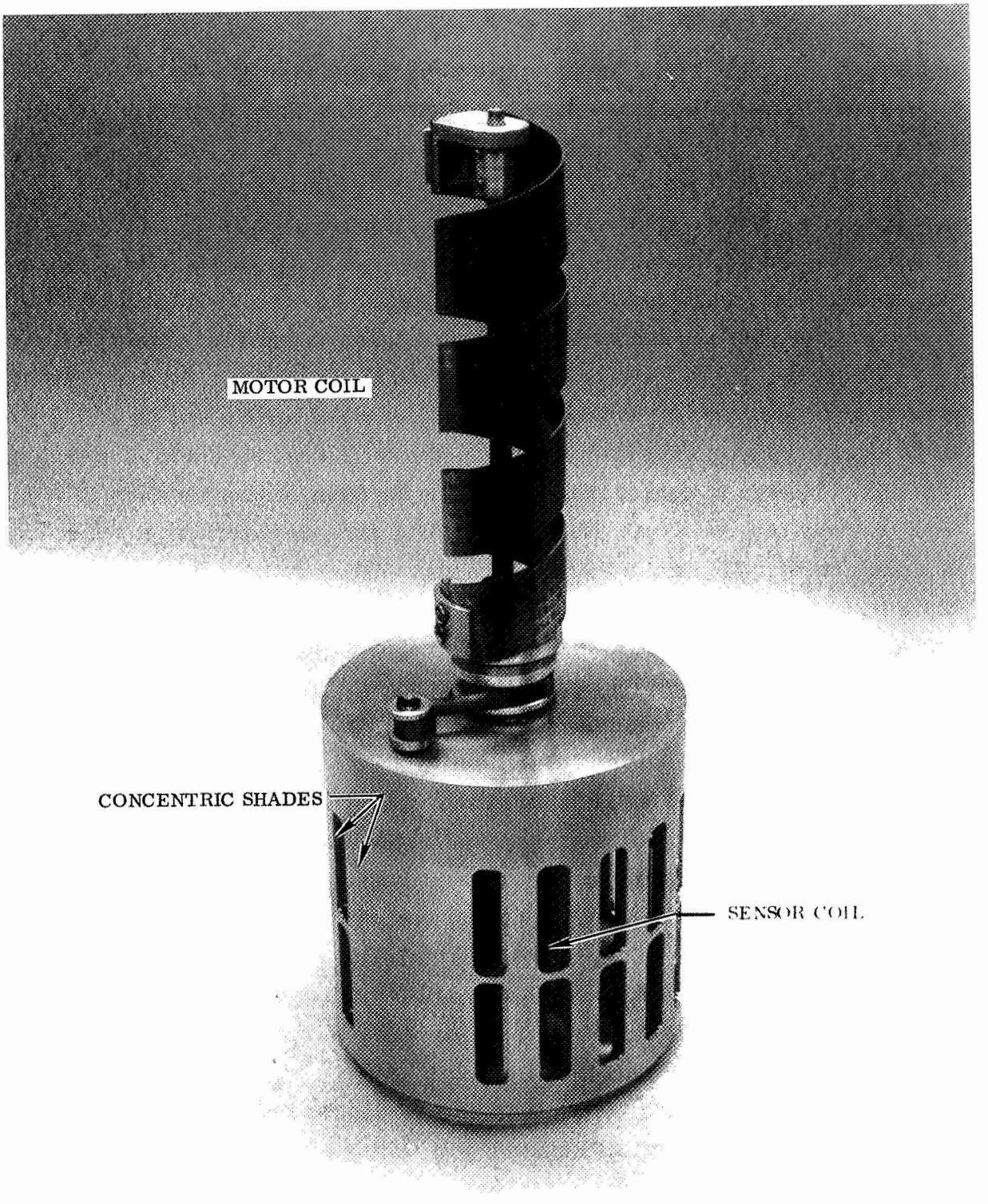

Fig. 13 Stored Energy Device (Prior to Thermal Coating)

in Fig. 14. The pawl works within an internal gear which is attached to the motor hub. Another pawl working on the same gear is fixed to the main shaft via a set screw mount.

Referring again to Fig. 13, it is evident that a cyclic rotation of the motor coil base will provide a unidirectional rotation to the motor hub. The hub runs in a set of single-row precision ball bearings which ride on the shaft. Reverse wound about the motor hub is a constant tension negator spring. The spring tension provides a constant torque on the outer shade. The moment arm is determined by the radius of the motor hub. Torque may be adjusted by several methods: (1) changing motor hub radius; (2) adding springs; or (3) changing spring width and thickness. The two concentric shades are aluminum with milled slots in 10-degree increments. On the outer concentric shade is a zone in which no slots have been cut. This is the lock-on slat and is parallel to the active side of a solar array. This slat then tracks the sun. Attached to the inside of the outer shade is an eighteen-tooth gear which serves as an escapement wheel (see Fig. 10). An escapement arm mounted at the top of the inside shade rides in a pair of single-row ball bearings and engages with the escapement wheel. Molydisulfide dry film lubricant on the wheel reduces frictional drag.

The escapement arm is actuated by the sensor coil. This coil is also P675-R, but is 0.010-inch thick for best thermal response. At the base, the coil is hard-mounted to the shaft. The top termination carries an actuator pin assembly which rides in ball bearings. Curved plates are used on coil terminations as in the motor coil. The base of the sensor coil may be rotated relative to the inside (fixed) shade. This provides a preload adjustment so that the coil may operate within a given temperature range. The coil, then, may be set to actuate the escapement at a specific temperature.

All bearings were cleaned in a sonic bath of MEK and flushed with alcohol after installation. Spacers on bearing races allowed only rolling contact on the bearings themselves. The only sliding contact was the escapement arm/wheel interface where molydisulfide lubricant was used. No lubricant was used in the ratchet assembly.

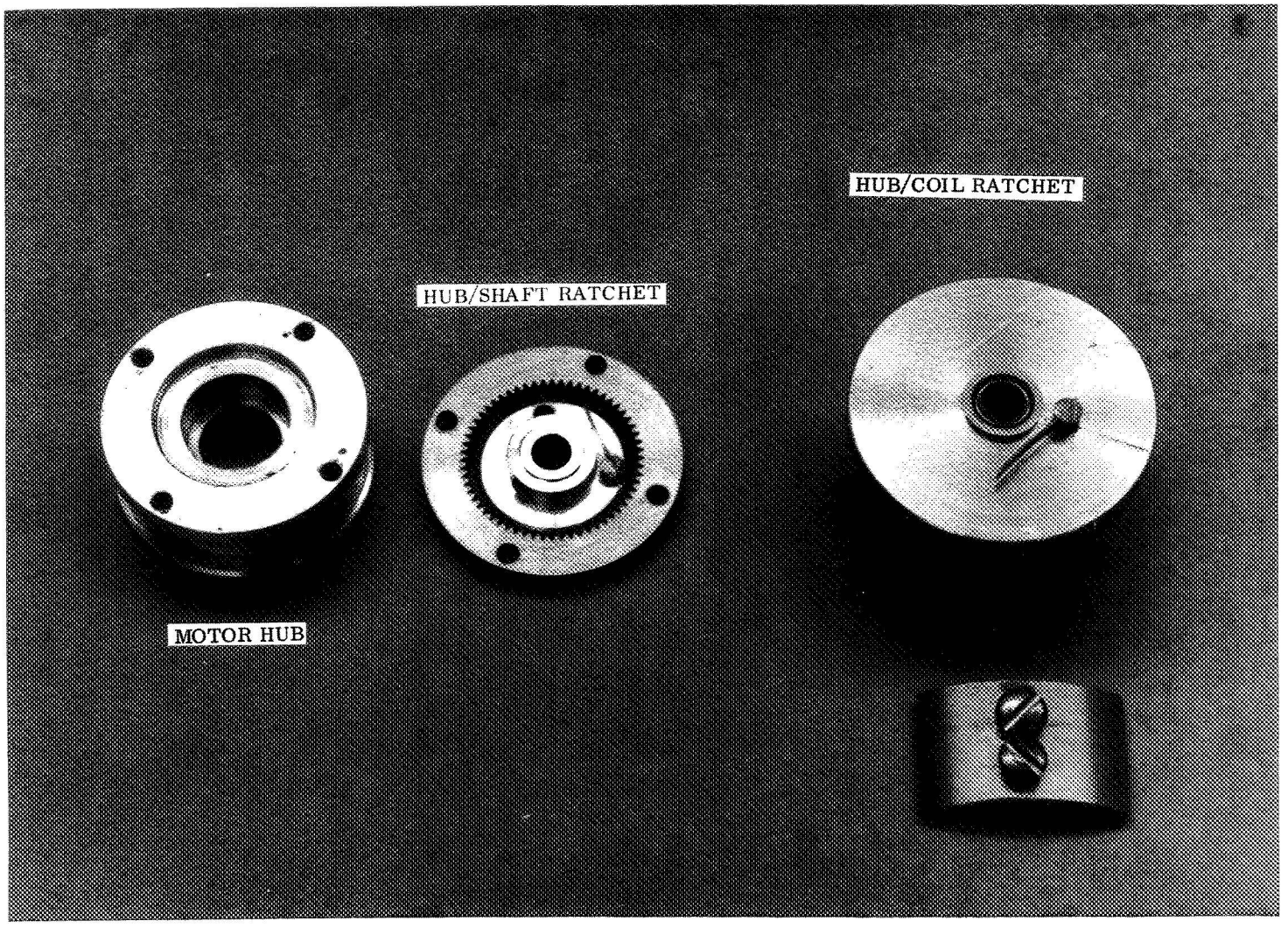

Fig. 14 Stored Energy Ratchet Assembly

C. PRELIMINARY TESTING

To check the operation of heliotrope models, preliminary thermal vacuum tests were performed on three models. These tests were conducted informally in a bell jar vacuum setup. The object was to identify "bugs" which might occur in final testing so that modifications could be made and procedures identified. The preliminary tests were inexpensive and will help prevent delays and downtime when final testing is performed in a controlled environment.

1. Summary of Tests

Three models were tested and in short, the results are as follows. The seasonal adjuster oriented itself to the light source from an orbitrary 40 degrees off-angle in 90 seconds to four minutes, depending on coil reflector configuration. Error angle was visibly less than 5 degrees. This device would provide adequate seasonal tracking for a solar array. The planetary gear device oriented itself to the light source from an off-angle of 90 degrees and provided tracking motion, as designed. Tracking motion was somewhat erratic because of an undersized coil. The stored energy device functioned as designed. It provided orientation capability from any degree of initial off-angle and 10 degree incremental sun tracking.

2. Test Setup

The experimental test setup for preliminary testing is illustrated in Fig. 15. A 36-inch diameter bell jar provided a vacuum environment of 8×10^{-5} to 2×10^{-4} torr. Pumpdown time was about 35 minutes. A cylindrical copper cooling shroud 16 inches in diameter was placed with its axis horizontal and at a 45-degree angle, with the 12-inch observation ports. Two colortran B10-32 lamps with parabolic reflectors were used as a sun simulator. The lamps were water cooled and provided a partially collimated light source. Intensity was checked in the test plane by a constant temperature secondary standard solar cell and related directly to lamp current. Simulator current was monitored throughout the tests and variation in the test area was within 10 percent. These lamps radiate more infrared energy than the solar source, so the intensity was

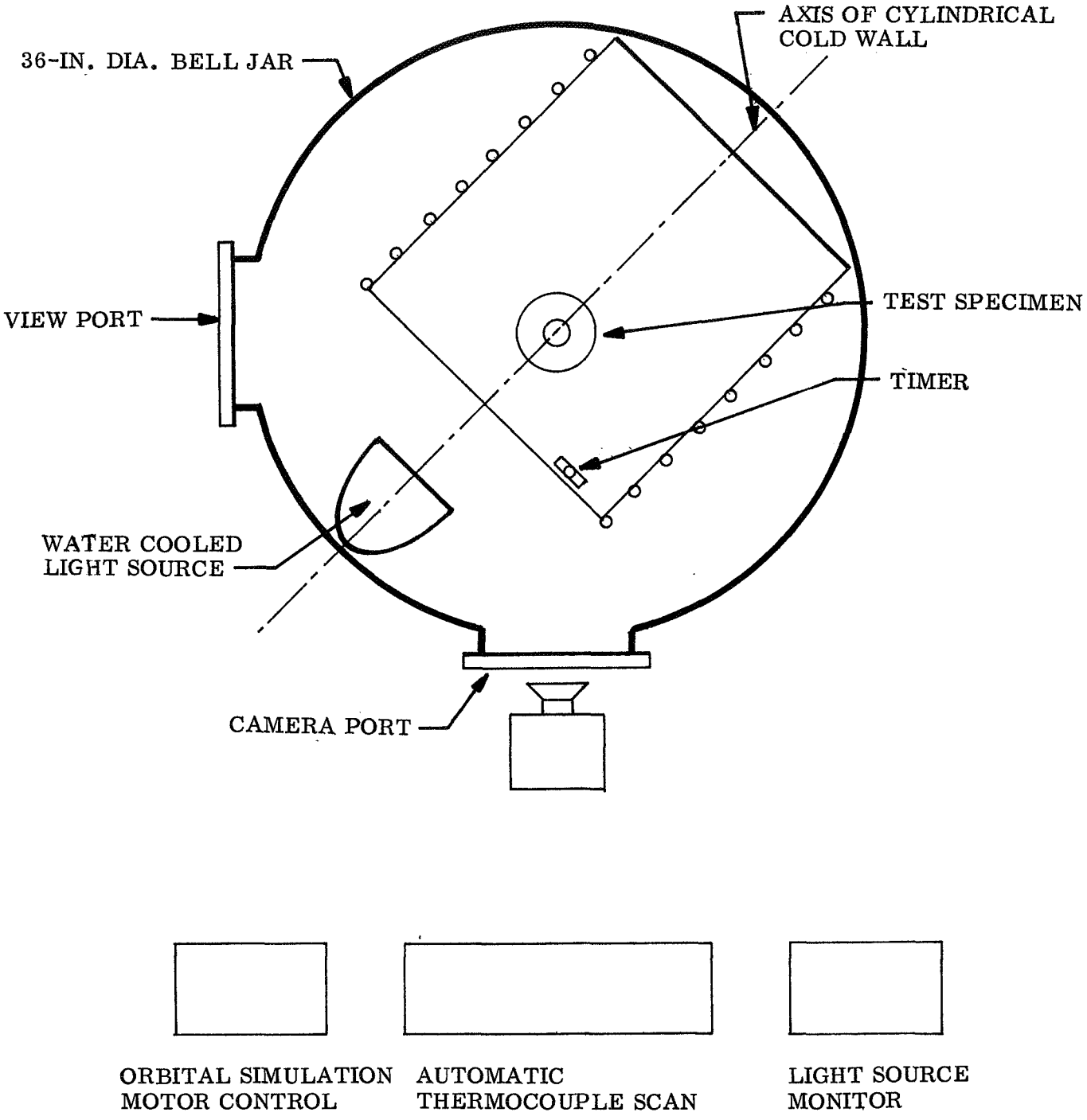

Fig. 15 Preliminary Test Setup

was possibly thermally higher than one sun. A DC gear-motor was used to allow in situ positioning of test specimens. The motor drove each model through a flex shaft arrangement and could be used to simulate an accelerated orbital rate (7 degrees per minute – synchronous rate is 0.25 degree per minute and 8100 nm orbiting vehicle is about 0.7 degree per minute). The motor had copper cooling straps to the LN_2 shroud to prevent overheating should it be used continuously. A pocket watch was installed in the chamber so that it provided a time reference in the test movie. Four thermocouples on each model, one on the motor, and one on the cooling shroud, were scanned continuously by a Honeywell Electronik-16 recorder. Time lapse photography was used to document specimen position versus time.

3. Model Tests

a. Seasonal Adjuster Test. Prior to the first Seasonal Adjuster test the device was installed in the chamber as shown in the photograph, Fig. 16. One mounting screw also served as an anchor for the stationary sun gear. Since this screw was not securely tightened, the sun gear was free to rotate, and the device would not move relative to the light source. Camera documentation shows only movement due to the positioning motor. Temperature records were obtained, however, and visual observation indicated a need for a shade extension to prevent illumination of both bimetal coils simultaneously. This situation would engage both coils and greatly hinder tracking due to binding. For the second seasonal adjuster test the sun gear was properly fastened and the shade modified to prevent illumination of both coils. A foil reflector was placed behind one coil to study its effect on coil heating rate. The reflector may be seen in photograph, Fig. 9, prior to test. Initially, the device was misoriented an angle of 40 degrees, as shown in Fig. 8(b). Upon illumination, the tracker oriented itself within 90 seconds of elapsed time. The device was then allowed to cool and motor driven to the position shown in Fig. 8(c). The simulator was turned on, and the device oriented itself fully in about 5 minutes (1.7 minutes to start rotation and 4 more minutes to fully orient). Film coverage was not available for the second test.

b. Planetary Gear Device. The device shown in photo Fig. 6 was placed in the chamber with an initial misorientation of 90 degrees. The device oriented itself in less than 60 seconds. The orbit simulation motor was then started, and the device tracked the light

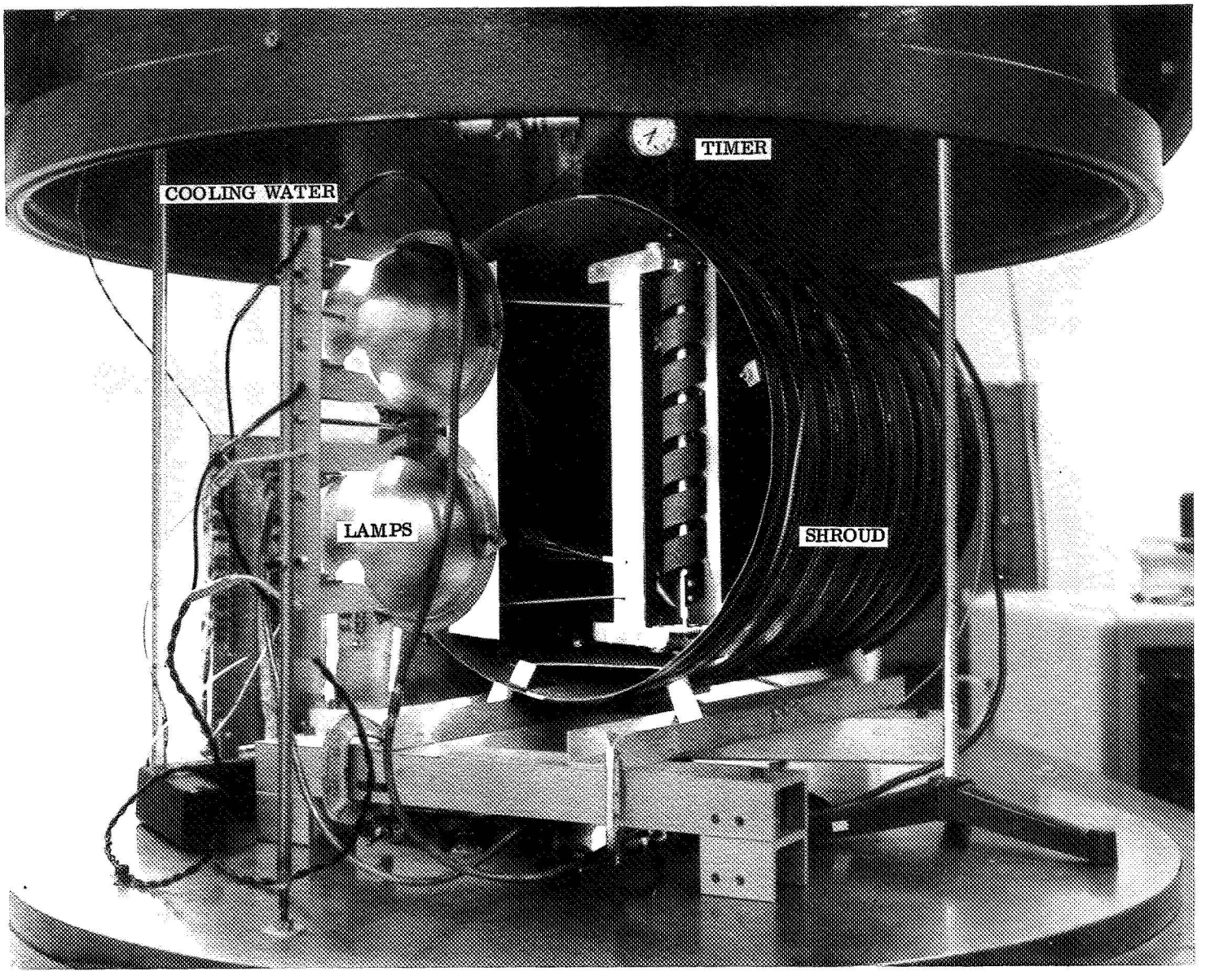

Fig. 16 Seasonal Adjuster in Test Chamber

source. Tracking action on this device, as witnessed by time lapse photography, was erratic because of an undersized bimetal coil. The torque capability of the thin coil was not adequate to provide smooth tracking, so a thicker coil will be incorporated for the final testing. No thermocouples were attached to this model.

c. Stored Energy Device. The stored energy device shown in Fig. 17 was initially misoriented 270 degrees from the light source. The simulator was turned on and a sun-seek function occurred in 10-degree increments for 60 degrees of rotation, at which point the test was terminated. Heat input from the simulator caused the small cooling shroud to warm from $-295^{o}F$ to $0^{o}F$ during the test period of 70 minutes. This reduced the sensor coil cooling rate and affected tracker response. A second test was run on the device after modifying the shroud slightly and a 60-hour vacuum soak at 10^{-4} torr. (See Fig. 18 for simulated altitude.) The device was misoriented 60 degrees before the simulator was started. Initial orientation rate was about 2 degrees of arc per minute for this particular model in the partial coldwall environment. The device oriented itself 60 degrees and locked on the light source. At this point the drive motor was started at an accelerated rate of seven degrees per minute to simulate array misorientation "turn" zone on Fig. 19. The device again started tracking. During all of the test operation temperatures are monitored. One readout is plotted in Fig. 19. The device again started tracking. On Fig. 19, the letter C indicates a closing of the shade assembly and 0 indicates an opening. The temperature plots are for thermocouples on the motor coil, sensor coil, outer shade, and coldwall shroud. Note the increase in shroud temperature caused by simulator heat input. Lamp current was varied to help control the effect of an imperfect cold wall. The motor coil performed as designed, providing a winding motion to the negator spring with temperature variations. Reference is made to the first quarterly report for an explanation of the theory and mode of operation of this device.*

---

*Passive Solar Array Orientation System, Second Quarterly Report, NAS 5-11637, 23 Dec 1968 – 23 Mar 1969, pg 45.

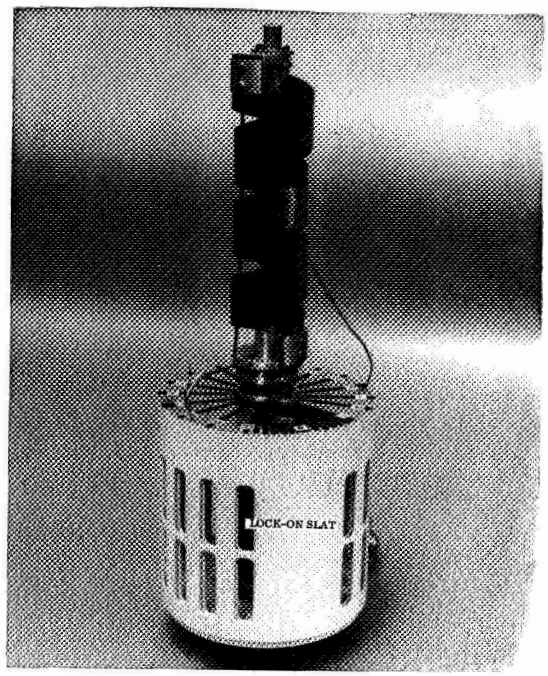

Fig. 17 Stored Energy Device (Test Configuration)

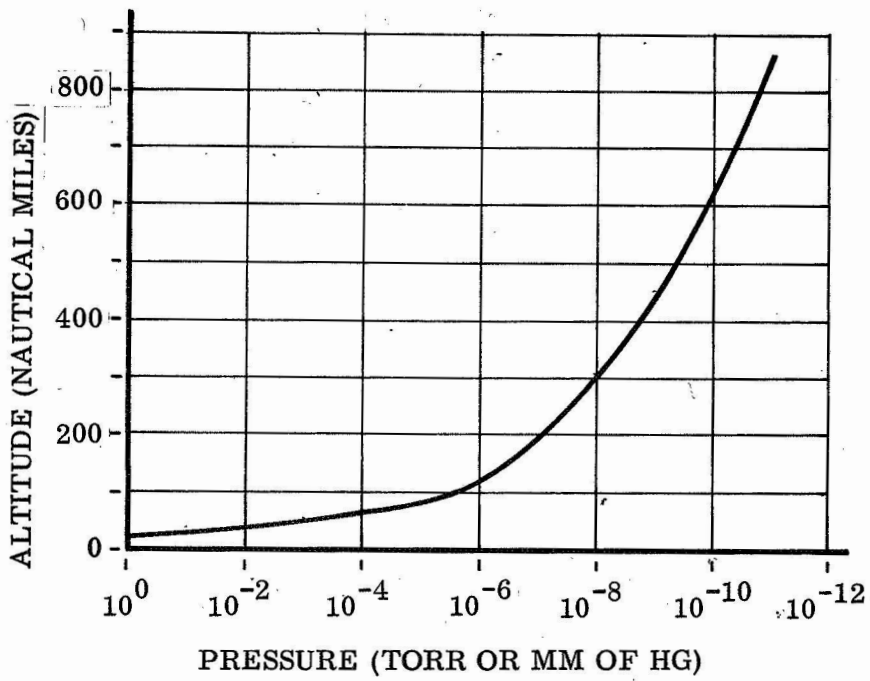

Fig. 18 Vacuum Chamber Simulated Altitude

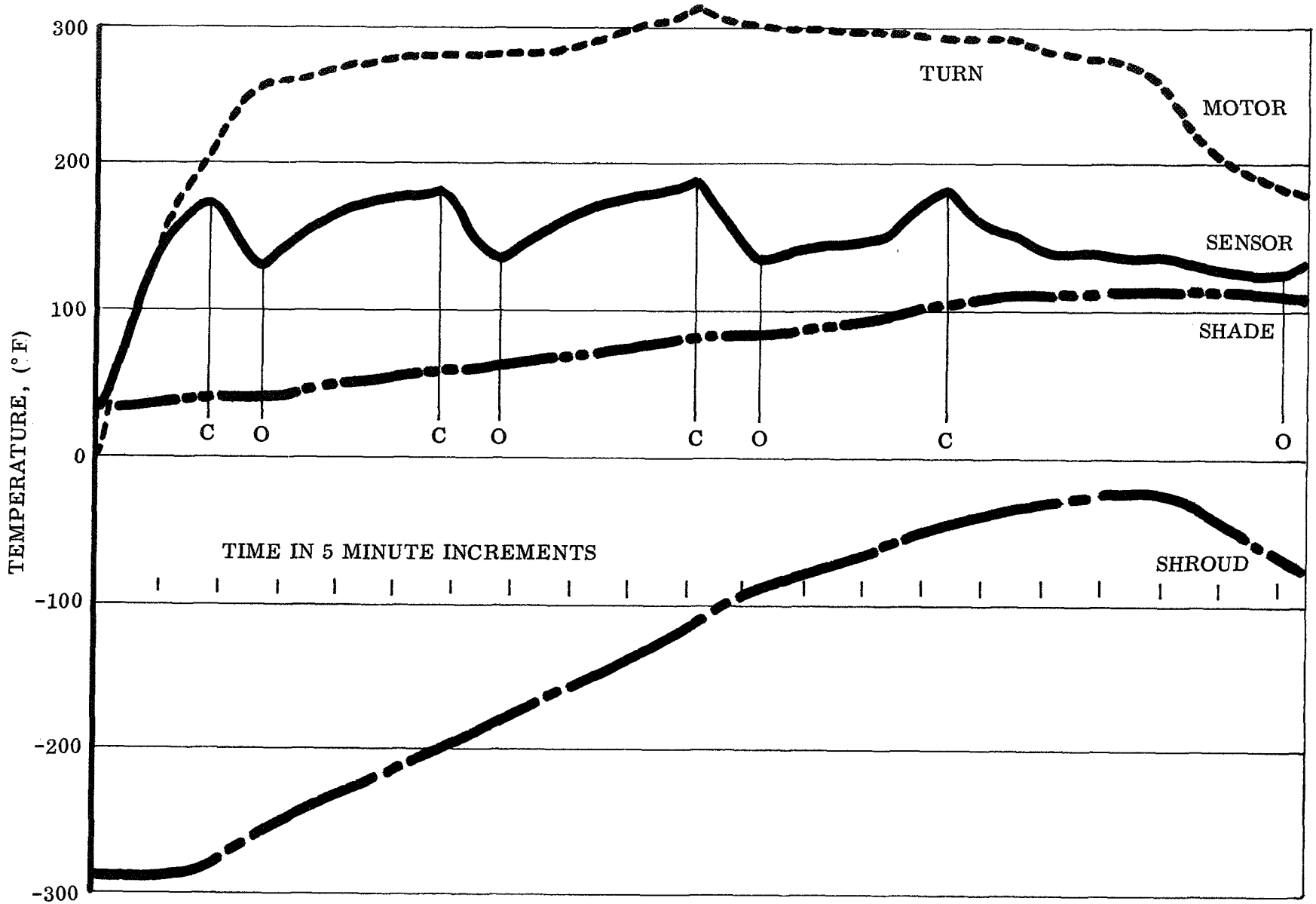

Fig. 19 Temperature Plot for Stored Energy Device

4. Test Configurations

Model	Seasonal Adjuster	Planetary Gear	Stored Energy
Coil Coating	A, B	A, B	E
Structure Coating	F	None	C
Shade Configuration	H	I	J
Reflector Configuration	J	None	None
Instrumentation	K	L	K, L

A. Yellow Zinc Chromate Primer, MIL-P-8585A (air dry)
B. 3M Velvet Coating, No. 101-C10 Black (baked on)
C. 2A-100 White Thermatrol, PB-105-101 (air dry)
D. Sonic Cleaning in MEK and Alcohol
E. LMSC Oxidization Treatment
F. Bare Sanded Aluminum
G. Foil Reflector Behind Coil
H. Closed Shade Support
I. Centered Shade
J. Concentric Cylinders
K. 4 Thermocouples on Model
L. Photo Coverage

SECTION III
NEW TECHNOLOGY

New technology reported during this quarterly period applies mainly to tracker device types. A two-coil continuous tracker has been devised for continuous tracking in intermediate to high orbit situations. Also for continuous tracking is a planetary shade device. These trackers are described in Section II.

A true heliotrope has been approximated using semi-circular bimetal coils mounted in series banks. This device favors no particular axis but follows the sun continuously. In addition, a method for eliminating axial motion from helical coils was developed. The new coil design is called the non-helical helix. Use of this type of coil allows smaller winding diameters and better volume packing considerations. These devices are also presented in Section II.

SECTION IV
PROGRAM FOR NEXT REPORTING PERIOD

The work to be performed during July, August, and September 1969 will constitute the third and final quarter of effort for the exploratory phase of this program (NAS5-11637). All contractural tasks will be completed during this period, with the exception of the final report which will be due 30 days after the end of the quarter. Modifications to existing conceptual models will be made and all models tested. The Task IV test results will be analyzed and conclusions presented. Task V documentation will consist of a 16-mm test film and a comprehensive final report (replacing a third quarterly). All program expenditures will be within contract scope and labor/cost allocations.

SECTION V
CONCLUSIONS AND RECOMMENDATIONS

1. Angular impulse limitations on some vehicles may dictate a non-incremental tracking device.

2. Bimetal elements appear to be extremely resistant to thermal cycling damage.

3. Bimetal coil linear motion may be eliminated by use of a non-helical helix. Coil winding diameters may also be minimized with this device and wider bimetal strips can be assembled.

4. A continuous tracking device was designed to supply more than adequate tracking torque by utilizing two motor coils; one coil is cooling while the other is providing tracking torque.

5. The work accomplished to date has demonstrated that simple, reliable passive solar array sun orientation drive systems are feasible.

Appendix A

THERMAL COOLING COMPUTER PROGRAM

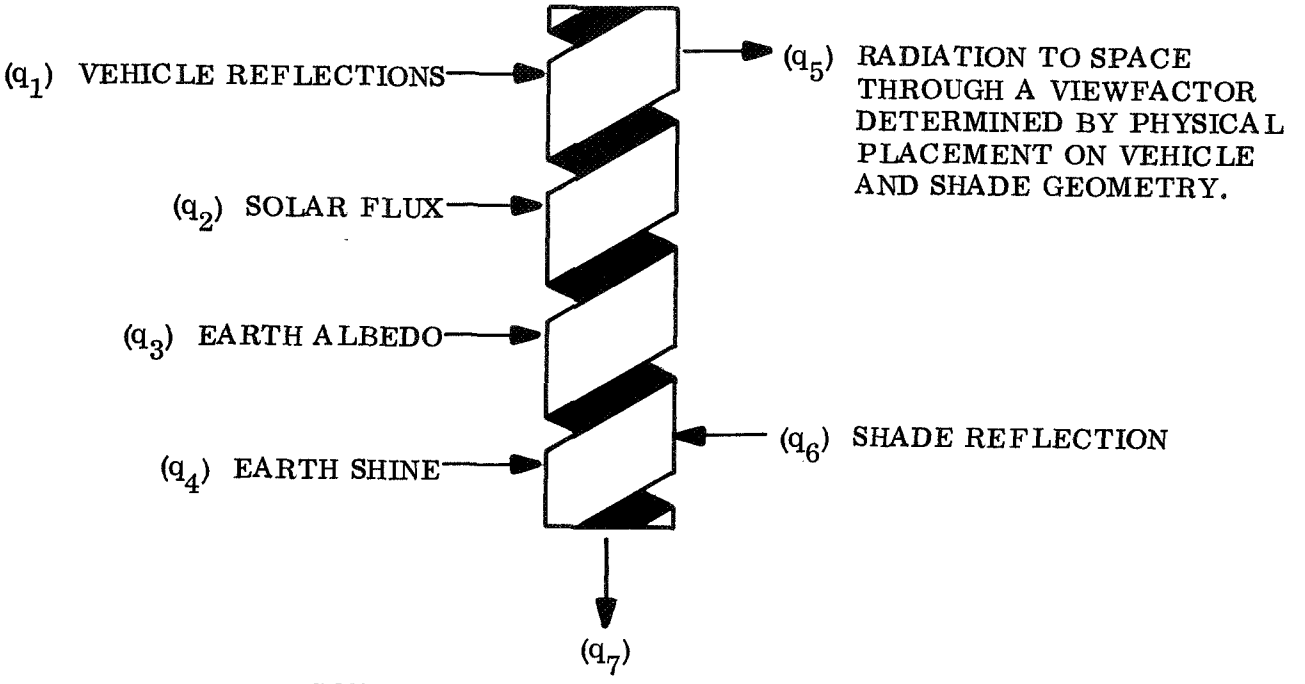

The heat fluxes shown above were simplified to consider only solar flux input and radiation to space zero sink output (q2, q5) for the purposes of calculation. The simplified equations give an indication of the relative merit of various α and ϵ values associated with thermal coatings.

A more realistic feeling for thermal response will be obtained by model testing, which can form the basis for a more rigorous thermal model of any given tracker if required.

The basic radiation heat transfer equation

$$Q = \sigma A \epsilon \left(T_c^4 - T_s^4 \right) \qquad \text{(A-1)}$$

was equated to the transient heat flow equation

$$Q = mc \frac{dT}{d\tau} . \tag{A-2}$$

As sink temperature, T_s, is ideally zero the expression for cooling time becomes

$$\tau = \frac{mc}{3\sigma A\epsilon} \left(\frac{1}{T_f^3} - \frac{1}{T_i^3} \right) . \tag{A-3}$$

T_i was taken as the upper equilibrium temperature with a one-sun solar flux input:

$$T_i = \left(\frac{\alpha}{\epsilon} \frac{SA_p}{A_t} \right)^{1/4} \tag{A-4}$$

Cooling time from the equilibrium temperature for a given temperature drop ΔT is given by

$$\tau = \frac{k\ tc}{\alpha\epsilon} \left(\frac{1}{(T_i - \Delta T)^3} - \frac{1}{(T_i)^3} \right) \tag{A-5}$$

Figure A-1 shows the computer program listing to obtain the data in Fig. A-2. Figure A-2 gives cooling time in minutes for a given temperature drop (DELTAT) as a function of α and ϵ from the upper equilibrium temperature. The equilibrium temperature is listed in degrees rankine below each time listing.

```
      C     IDEAL RADIATIVE COOLING TIME CALCULATIONS FOR BIMETAL COIL VS.
      C     THERMAL COATING PROPERTIES
      C     NOTATION  TAU=TIME,MINUTES  THICK=STOCK THICKNESS,INCHES  ABSOR=
      C     ABSORBTIVITY  EMISS=EMISSIVITY  AREAR=AREA RATIO (PROJECTED TO
      C     TOTAL)
            DIMENSION THICK(20),EMISS(20),ABSOR(20),DELTAT(20),TAUC(20),TE(20)
            TEQUIB (AB,SOLAR,EM,SIGMA,AREAR)=(AB/EM*SOLAR/SIGMA*AREAR)**.25
            SOLAR = 444.
            AREAR = .319
            SIGMA = 1.714 E -9
            RHO = .28
            CP = .12
            F = 2880.
            DATA IMAX,JMAX,KMAX,LMAX/5,11,11,11/
      4     FORMAT (17X,11F10.3)
       5    FORMAT  (1X,6HEMISS=,F4.2,6X,11F10.3)
       6    FORMAT (10X,7HABSOR=,11F10.3//)
          7 FORMAT  (1X,3X,7HDELTAT=,F5.1)
      99    FORMAT (10X,11F6.4)
      98    FORMAT (10X,11F5.0)
          8 FORMAT(1H1,6HTHICK=,F4.3)
            READ(5,99)  (THICK(I),I=1,IMAX)
            READ(5,99)  (ABSOR(L),L=1,LMAX)
            READ(5,99)  (EMISS(K),K=1,KMAX)
            READ (5,98) (DELTAT(J),J=1,JMAX)
            DO 11 I=1,IMAX
            WRITE (6,8) THICK(I)
            DO 22 J=1,JMAX
            WRITE (6,7) DELTAT(J)
            WRITE (6,6) (ABSOR(L),L=1,LMAX)
            DO 33 K=1,KMAX
            DO 44 L=1,LMAX
            AB=ABSOR(L)
            EM=EMISS(K)
            FACTOR = F/SIGMA*RHO/EMISS(K)*THICK(I) *CP
            TAU=((1./(TEQUIB(AB,SOLAR,EM,SIGMA,AREAR)-DELTAT(J))**3)-(1./TEQUI
           CB(AB,SOLAR,EM,SIGMA,AREAR)**3))*FACTOR
            TAUC(L)=TAU
            TE(L)=TEQUIB(AB,SOLAR,EM,SIGMA,AREAR)
      44    CONTINUE
            WRITE (6,5) EMISS(K),(TAUC(L),L=1,LMAX)
            WRITE (6,4) (TE(L),L=1,LMAX)
      33    CONTINUE
      22    CONTINUE
      11    CONTINUE
            END

END OF LISTING,     0 *DIAGNOSTIC* MESSAGE(S).
```

Fig. A-1 Coil Cooling Time Program

THICK=.015

DELTAT= 25.0

ABSOR=	.050	.100	.200	.300	.400	.500	.600	.700	.800	.900	1.000
EMISS= .05	16.926	8.331	4.111	2.723	2.033	1.622	1.348	1.153	1.007	.894	.804
	536.155	637.600	758.238	839.129	901.702	953.434	997.898	1037.105	1072.311	1104.355	1133.831
EMISS= .10	17.249	8.463	4.165	2.755	2.056	1.638	1.361	1.164	1.017	.902	.811
	450.851	536.155	637.600	705.620	758.238	801.739	839.129	872.098	901.702	928.648	953.434
EMISS= .20	17.647	8.624	4.231	2.794	2.083	1.659	1.377	1.177	1.028	.912	.819
	379.119	450.851	536.155	593.353	637.600	674.180	705.620	733.344	758.238	780.897	801.739
EMISS= .30	17.922	8.736	4.277	2.821	2.101	1.673	1.388	1.186	1.035	.918	.825
	342.573	407.390	484.471	536.155	576.136	609.190	637.600	662.651	685.146	705.620	724.453
EMISS= .40	18.140	8.823	4.312	2.842	2.116	1.683	1.397	1.193	1.041	.923	.829
	318.800	379.119	450.851	498.949	536.155	566.915	593.353	616.666	637.600	656.654	674.180
EMISS= .50	18.323	8.897	4.342	2.860	2.128	1.693	1.404	1.199	1.046	.928	.833
	301.502	358.549	426.389	471.877	507.064	536.155	561.159	583.207	603.005	621.025	637.600
EMISS= .60	18.484	8.961	4.368	2.875	2.138	1.700	1.410	1.204	1.051	.931	.836
	288.068	342.573	407.390	450.851	484.471	512.266	536.155	557.221	576.136	593.353	609.190
EMISS= .70	18.627	9.018	4.391	2.888	2.148	1.707	1.416	1.209	1.054	.935	.839
	277.178	329.622	391.989	433.807	466.156	492.900	515.886	536.155	554.356	570.922	586.160
EMISS= .80	18.757	9.070	4.412	2.901	2.156	1.714	1.421	1.213	1.058	.938	.842
	268.078	318.800	379.119	419.564	450.851	476.717	498.949	518.552	536.155	552.178	566.915
EMISS= .90	18.876	9.118	4.431	2.912	2.164	1.720	1.426	1.217	1.061	.940	.844
	260.299	309.549	368.118	407.390	437.769	462.884	484.471	503.506	520.598	536.155	550.465
EMISS=1.00	18.988	9.162	4.449	2.922	2.171	1.725	1.430	1.220	1.064	.943	.846
	253.532	301.502	358.549	396.799	426.389	450.851	471.877	490.417	507.064	522.217	536.155

DELTAT= 50.0

ABSOR=	.050	.100	.200	.300	.400	.500	.600	.700	.800	.900	1.000
EMISS= .05	37.514	18.140	8.823	5.801	4.312	3.428	2.842	2.426	2.116	1.875	1.683
	536.155	637.600	758.238	839.129	901.702	953.434	997.898	1037.105	1072.311	1104.355	1133.831
EMISS= .10	39.072	18.757	9.070	5.946	4.412	3.502	2.901	2.474	2.156	1.910	1.714
	450.851	536.155	637.600	705.620	758.238	801.739	839.129	872.098	901.702	928.648	953.434
EMISS= .20	41.068	19.536	9.378	6.126	4.535	3.594	2.973	2.533	2.206	1.953	1.751
	379.119	450.851	536.155	593.353	637.600	674.180	705.620	733.344	758.238	780.897	801.739
EMISS= .30	42.502	20.089	9.595	6.252	4.621	3.658	3.023	2.574	2.240	1.982	1.777
	342.573	407.390	484.471	536.155	576.136	609.190	637.600	662.651	685.146	705.620	724.453
EMISS= .40	43.667	20.534	9.768	6.353	4.689	3.709	3.063	2.607	2.268	2.005	1.797
	318.800	379.119	450.851	498.949	536.155	566.915	593.353	616.666	637.600	656.654	674.180
EMISS= .50	44.670	20.915	9.915	6.438	4.747	3.751	3.097	2.634	2.290	2.025	1.814
	301.502	358.549	426.389	471.877	507.064	536.155	561.159	583.207	603.005	621.025	637.600
EMISS= .60	45.562	21.251	10.044	6.512	4.797	3.789	3.126	2.658	2.310	2.042	1.829
	288.068	342.573	407.390	450.851	484.471	512.266	536.155	557.221	576.136	593.353	609.190
EMISS= .70	46.373	21.555	10.161	6.579	4.843	3.822	3.152	2.680	2.328	2.057	1.842
	277.178	329.622	391.989	433.807	466.156	492.900	515.886	536.155	554.356	570.922	586.160
EMISS= .80	47.121	21.833	10.267	6.640	4.884	3.853	3.176	2.699	2.345	2.071	1.854
	268.078	318.800	379.119	419.564	450.851	476.717	498.949	518.552	536.155	552.178	566.915
EMISS= .90	47.819	22.092	10.365	6.696	4.922	3.881	3.198	2.717	2.360	2.084	1.865
	260.299	309.549	368.118	407.390	437.769	462.884	484.471	503.506	520.598	536.155	550.465
EMISS=1.00	48.476	22.335	10.457	6.749	4.958	3.907	3.219	2.733	2.373	2.096	1.876
	253.532	301.502	358.549	396.799	426.389	450.851	471.877	490.417	507.064	522.217	536.155

DELTAT= 75.0

ABSOR=	.050	.100	.200	.300	.400	.500	.600	.700	.800	.900	1.000
EMISS= .05	62.810	29.771	14.251	9.296	6.875	5.445	4.502	3.835	3.338	2.954	2.648

Fig. A-2 Cooling Time Printout

Appendix B

ROTATIONAL INERTIA NOMENCLATURE

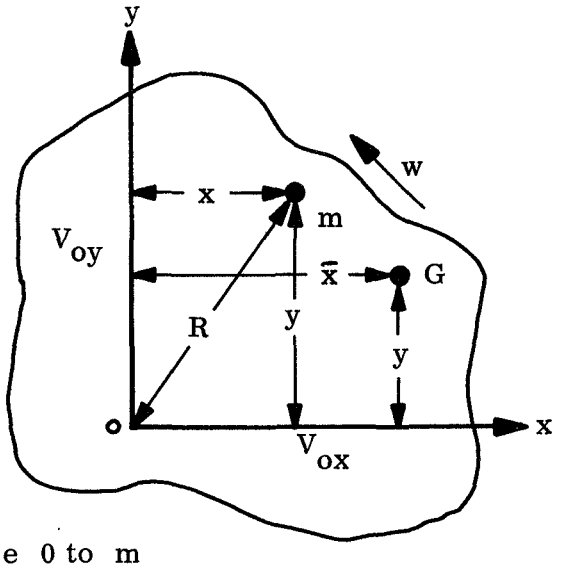

R = distance 0 to m

w = angular velocity

G = center of mass

m = particle of mass

v = velocity of m

o = reference point

x = distance to m along x axis

y = distance to m along y axis

$\bar{x}$ = distance to G along x axis

$\bar{y}$ = distance to G along y axis

$\bar{I}$ = moment of inertia about G

M = total mass

$$Ho = \Sigma m\ R^2\ w + \Sigma m\ Voy\ X - \Sigma m\ Vox\ y$$

and width the definition of moment of inertia about 0.

$$Ho = Io\ w + \bar{x}\ M\ Voy - \bar{y}\ M\ Vox$$